Architecture and Tectono-magmatic Evolution of the Campos Rifted Margin: Control of OCT Structure by Basement Inheritance

Natasha Stanton[1], Nick Kusznir[2], Andres Gordon[3] & Renata Schmitt[4]

[1]State University of Rio de Janeiro, Brazil

[2]University of Liverpool, UK

[3]AC-GEO Consulting

[4]Federal University of Rio de Janeiro, Brazil

ABSTRACT

The formation of rifted margins involves the deformation of pre-existing lithosphere whose rheological and mechanical behavior during extension is complex since it is the product of numerous earlier tectonic events. In this work we investigate the Campos Rifted Margin (CRM) architecture, with the aim of exploring the role of basement inheritance and early magmatism on margin evolution. We present a new compilation of high resolution aeromagnetic data, integrated with seismic interpretation and crustal thickness from 3D gravity inversion, to resolve margin architecture, ocean-continent transition (OCT) structure and the oceanward extent of continental basement. We examine the lateral variation of crustal rheology, necking geometry and rift segmentation, revealing striking spatial heterogeneities that separate three distinct sectors along the Campos margin. The basement of the Campos Rifted Margin consists of Precambrian/Eo-Paleozoic Ribeira Belt (RB) and the easternmost Cabo Frio Tectonic Domain (CFTD) whose Neoproterozoic-Cambrian nappes and thrusts are well preserved offshore and give a rheologically layered crust. This pre-rift basement configuration, along with the Mesozoic magmatism, has resulted in different crustal responses to extension which vary from north to south. It influenced the temporal and spatial distribution of deformation, and as a consequence, the necking geometry, subsidence and sedimentary evolution of the margin. We show that the Campos basin evolution was controlled by crustal inheritance corresponding to that observed in onshore basement terranes. The more massive basement of the northern Campos basin can be correlated with the post-collisional Cambro-Ordovician magmatic province of the Aracuai belt that partially obliterated the earlier orogenic structures. The lack of a structured crust localized the strain generating the observed narrow necking zone. In addition, its more mafic composition resulted in a competent crust which also influenced the rifting processes. In contrast the basement of the central and southern Campos margin, represented by the Cabo Frio Tectonic Domain, is structurally and petrologically distinct from the Aracuaí Belt and has layered orogenic crust which responded differently to rifting stresses forming the observed wide necking zone. We propose that the Campos Rifted Margin evolved from a pre-rift complex inherited rheology which dominated the first stages of rifting. However once the crust was highly extended, the deformation was nearly synchronous regionally, leading to giant salt basin formation and breakup.

1. Introduction

The way in which continental lithosphere deforms in response to tectonic stresses is a consequence of its rheology and thermal state (Kusznir and Park, 1987). Continental accretion processes produce a complex lithospheric architecture, with diverse compositional domains, which have different rheological and mechanical behaviors during continental breakup and rifted margin formation. In order to examine such complexity, it is important to understand the initial pre-rift conditions. However this is usually difficult to access since margins lie in deep water with limited basement drill data. Several previous studies have focused on the role of inheritance during continental breakup using both direct and indirect observations (Chenin et al., 2015). It has been proposed that inheritance plays an importance role in controlling the formation of rifted margins, defining the distribution and localization of deformation, the ocean-continent transition (OCT) architecture and magmatism (Dunbar and Sawyer, 1989; Allemand and Brun, 1991; Tomasi and Vauchez, 2001).

Numerical and analog models show that the pre-rift condition of the lithosphere directly affects its response to extension (Corti et al., 2010), exerting first-order control on the thinning process (Duretz et al., 2016) and guiding the crustal faulting style (Cappelleti et al., 2013; Brune et al., 2016). According to Huisman and Beaumont (2010) variations in depth-dependent extension can result from different lithosphere rheologies. Studies suggest that the brittle/ductile ratio controls the formation of wide versus narrow rifts (Buck, 1991; Sutra and Manatschal, 2012), ductile layer flow can determine where rift basins form at the surface (Whitmarsh and Manatschal, 2012), and the presence of magmatism (underplating) may influence strain localization (Callot et al., 2002; Gernigon et al., 2004; Yamasaki and Gernigon, 2009) and subsidence. The thermal structure of the lithosphere at the time of rifting and the kinematics in relation to basement fabric also fundamentally influence the final rift architecture (Brune et al., 2016).

The Campos Basin, located on the Southeastern Brazilian margin of the South Atlantic (Fig. 1), formed during Early Cretaceous rifting of western Gondwana. Its initial evolution is regionally well constrained (Guardado et al., 1989; Chang et al., 1992), although a detailed investigation of spatial crustal architectural variations is lacking. Its pre-breakup history involves a complex geological evolution where the lithosphere registered successive tectonic cycles, creating an initial pre-rift “canvas” which is not a simple compositional or rheological layer-cake.

This paper presents new geophysical data that highlights the crustal structure, segmentation and magmatism of the Campos rifted margin. Our results reveal differences from south to north in OCT structure and volcanism which are related to changes in breakup deformation, lithospheric inheritance and regional plate kinematics. We present evidence of deep crustal discontinuities and magmatism and discuss their implications for the evolution of the SE Brazilian Margin.

2. Campos margin geological framework

2.1 The crystalline basement

The Campos margin basement developed over Precambrian-Early Paleozoic terranes, well constrained onshore, known as the Ribeira/Araçuai belts and the Cabo Frio Tectonic Domain (CFTD) (Fig. 1).

During the Neoproterozoic-Cambrian amalgamation of western Gondwana blocks, the convergence of the São Francisco and Congo/Angola cratons formed the Ribeira and Araçuai orogenic belts (Fig. 1). Although Ribeira (transpressional) and Araçuaí (westward thrust of allochthonous units) have differences in tectonic fabric (NE-SW and N-S oriented respectively – following the São Francisco craton boundary, Fig. 1) and strain regimes, they were formed during the same tectonic events (ca. 0.65 – 0.5 Ga), and can be considered as two segments of the same orogenic belt (Heilbron et al., 2004; Pedrosa Soares et al., 2001, Degler et al., 2017; Egydio-Silva et al., 2018). Both belts exhibit similar pressure and thermal metamorphic regimes (granulite and amphibolite facies), and display structural continuity without a clear boundary between them (Egydio-Silva et al., 2018 - Fig. 1). One striking difference among the belts is the large volume of Cambro-Ordovician magmatism on the Aracuaí sector, representing a late to post tectonic environment (De Campos et al., 2016).

In addition, the Ribeira belt shows two distinct domains: Occidental and Oriental (Heilbron et al 2004 – Fig. 1). The Occidental terrane is comprised of Paleoproterozoic basement and Neoproterozoic supracrustals deformed and metamorphosed, interpreted as the paleomargin of the Sao Francisco Craton reworked during the Brasiliano events. The Oriental terrane, to the east, is comprised only of Neoproterozoic units, mostly supracrustals intruded by magmatic rocks from 620-480 Ma (Fig. 1). Both terranes have a NE-SW structural grain and a metamorphic pattern of high temperature and low pressure. Heilbron et al. (2004) defines a suture zone in between these domains, the Central Tectonic Boundary (Fig. 1).

The Cabo Frio Tectonic Domain (CFTD), east of the Ribeira Belt, has contrasting characteristics when compared to the Oriental Terrane (Fig. 1). It has no Neoproterozoic-Cambrian magmatic rocks, being comprised of Paleoproterozoic gneisses (ca. 2.0 Ga) tectonically interleaved in a ductile regime with Neoproterozoic gneisses (ca. 0.6 Ga). Both units were metamorphosed at higher pressure than the Oriental Terrane, ca. 14 kbar, in the same temperature conditions, ca. 850 ^{o}C . The tectonic event that affected the CFTD occurred at the end of the Neoproterozoic and the beginning of the Cambrian (ca. 0.54-0.50 Ga - Schmitt et al., 2004), 50 My younger than the Ribeira belt. The structural grain of the CFTD is oriented NW-SE, orthogonal to the rest of the Ribeira belt (Fig. 1). The Neoproterozoic unit of volcano-sedimentary protoliths display penetrative foliation with several generations of folding. The Paleoproterozoic rocks, with plutonic protoliths, developed deformation partitioning with low strain sectors preserving primary igneous structure. Near the contacts with the Neoproterozoic gneisses, these Paleoproterozoic rocks are foliated, folded and partially melted (migmatites). These contacts are interpreted as fold nappes and high strain shear zones that superpose the Neoproterozoic meta volcano-sedimentary rocks over the Paleoproterozoic basement (Schmitt et al., 2016).

All these differences between the CFTD and the Oriental Terrane are interpreted as indicating that these terranes represent distinct tectonic plates at the end of the Neoproterozoic separated by a suture zone (Schmitt et al., 2016 – Cabo Frio Tectonic Limit-Fig. 1). The last continental collision event, the Buzios Orogeny, is considered to result from the closure of an oceanic domain due to a subduction towards the NW, suturing the São Francisco and Congo/Angola cratons during Gondwana amalgamation (Schmitt et al., 2004, 2016). The Paleoproterozoic gneisses of the CFTD are interpreted as the paleomargin of the Congo-Angola craton.

In summary, the Cabo Frio Tectonic Domain is distinct from the rest of the Ribeira\Araçuaí belts (Fig. 1) and it has been proposed that they represent different tectonic plates that amalgamated in the Neoproterozoic during the Buzios Orogeny (Schmitt et al., 2016).

2.2. The sedimentary record

The stratigraphic record of the Campos Basin is divided into three main units (Chang et al., 1992; Winter et al., 2007). The Rift section is represented by three sequences from the Hauterivian to Early Aptian, comprising up to 5000 m of volcanic and sedimentary rocks. The Hauterivian sequence is composed of volcanic rocks (Cabiunas Fm.) and minor silicilastic rocks. The Barremian to Early Aptian rift sequences are siliciclastic deposits, lacustrine carbonates and shales (Lagoa Feia Gr.), the latter considered to be the main source rock and the carbonates considered to be a good reservoir for hydrocarbons. The late-rift stage consists of Middle to Late Aptian transitional siliciclastic and carbonates rocks (the pre-salt reservoirs), and evaporites (Retiro Fm.), which exhibit pillows, domes and salt wall structures (Winter et al., 2007). The post-breakup drift sequences were greatly affected by salt tectonics (Winter et al., 2007) and magmatism, comprising: (1) Albian–Cenomanian carbonates and silicilastic sediments deposited in a neritic environment; (2) a transgressive marine system, from Turonian to Eocene, of siliciclastic rocks and marls; and (3) coarse-grained sandstones, platform carbonates and distal mudstone sedimentary beds (Chang et al., 1992).

2.3. Onshore and offshore Meso-Cenozoic magmatism

On the Southeast Brazilian margin, the onset of rifting at the Early Cretaceous was accompanied by extrusive and intrusive magmatism, recorded as tholeiitic dike swarms onshore (Deckart et al., 1998; Guedes et al., 2005; Valente et al., 2007) and flood-basalt at the base of the rift sequence offshore (Misuzaki et al., 1998; Fodor et al., 1984; Guardado et al., 1989; Lobo, 2007) (Fig. 2). The Campos Basin recorded a secondary magmatic cycle during the Upper Cretaceous-Early Tertiary (Misuzaki et al., 1992); at the Cabo Frio High it is represented by volcanic plugs, dikes and intrusive bodies (Oreiro et al., 2008). The age span of Campos Basin basalts attest for recurrent magmatism, with peak activity between 128-120 Ma, coeval with early crustal extensional events (Savastano et al., 2017).

Recent isotopic, geochemical and chronological analyses suggest that the sources for Campos basin basalts are compatible with an enriched mantle, that might be related to Neoproterozoic subduction and associated sediment metasomatism (EM1 mantle source of Zindler and Hart, 1986), during Gondwana amalgamation (Lobo, 2007; Carvas, 2016). Valente et al. (2007)

propose a distinct mantle for the CFTD, in relation to the Oriental Terrane, based on distinct geochemistry of the basic Cretaceous magmas.

At the conjugate Angola margin in the onshore Kwanza Basin there is evidence of magmatism dated from 131-126 Ma (Marzolli et al., 1999) which is coeval with the Campos Basin and adjacent Serra do Mar magmatism (Deckart et al., 1998; Siedner and Mitchel, 1975), indicating a regional magmatic event during early rifting.

3. Data and methods

3.1. Magnetic anomaly data

The magnetic data used in this work comprises eight different aerosurveys (see supplementary material Fig. S1 for survey location) from the Agência Nacional de Petróleo (ANP) public domain database. The data processing was carried out using Oasis Montaj V9.0. The individual survey acquisition parameters are: App040 (1969, 300 m flight height, variable line spacing and direction); CPRM-RJ (1978, 150 m flight height, N-S direction, 1000 m line spacing); App270 (1999, 500 m flight height, 3000 m line spacing, N30^{o}W direction); Mag1 (2002) and Mag2, EMAG01-BS-500 and EMAG01-BS-400 (1999, 150 m flight height, 1000 m line spacing, N30^{o}W direction); EMAG01-BM-S-4 (1999, 300 m flight height, other parameters same as previous survey.

Due to their acquisition differences, each survey was treated separately for removal of the Regional Magnetic Field (IGRF models). Afterwards they were leveled, re-projected to the same coordinate system, interpolated at 500 x 500 m interval and individually upward continued to 500 m altitude. Finally, all grids were knitted together using the suture method, trending to each other. The result consists of a high resolution total magnetic anomaly grid (Fig. 3a). As the available aerodata is insufficient to cover regionally the study area, we have filled the distal margin gaps with the marine magnetic data of Quesnel et al. (2009), upward continued at 500 m altitude (Fig. 3a).

In order to enhance lateral contrasts and separate shallow from deep sources, we have applied various transformations. We have upward continued the magnetic field to 10 km height (Fig. 3b) to eliminate short wavelengths associated with shallow sources. We determine the tilt angle (Miller and Singh, 1994), consisting of the ratio of the vertical and horizontal derivatives, for identifying regional trends (Fig. 3c) so that both deep and shallow sources are equally represented. We also show the analytic signal map which is useful to help locate magnetic sources (Fig. 3d).

3.2. Seismic data and wells

The Campos Basin seismic reflection data set comprises approximately 50 long-offset 2D seismic lines and 30 exploratory wells, courtesy of ANP. To illustrate the crustal architecture we selected three key regional seismic sections (Northern, Central and Southern transects) (locations in Fig. 1). Seismic attributes and post-stack processing techniques were applied consisting of structurally oriented filters, instantaneous amplitude and semblance. The depth

conversion of the interpreted seismic horizons made use of the following values compiled from well sonic logs and check shot information: 1) constant velocity of 2800 m/s for the sedimentary section, 2) constant velocity of 4200 m/s for the salt layer, 3) a vertical proportional distribution of interval velocities ranging from 3800 to 7800 m/s for the rift and basement units.

3.3 Gravity inversion

Regional crustal basement thickness has been determined using 3D gravity inversion which is carried out in the spectral domain and incorporates a lithosphere thermal gravity anomaly correction. The gravity inversion technique used is described in detail in Chappell and Kusznir (2008) and Alvey et al. (2008). It is important to include a correction for the lithosphere thermal gravity anomaly because of the elevated geotherm of ocean basin and rifted continental margin lithosphere; failure to do so leads to an over-estimate of Moho depth and crustal basement thickness. Applications of this gravity inversion technique to investigate rifted margin OCT structure are described in Cowie et al. (2015) for the Iberian margin and Cowie at al. (2015, 2016) for the Angolan margin.

Maps of regional free-air gravity anomaly and the resulting map of crustal basement thickness derived from gravity inversion, using public domain input data, are shown in Fig. 4. This input data consists of bathymetry (Smith and Sandwell, 2009), satellite free air gravity anomaly (Sandwell and Smith, 2009) and sediment thickness (Divins, 2003). Of these input data, the least reliable is the sediment thickness. The lithosphere thermal gravity anomaly correction requires information on the cooling age of ocean and rifted continental margin lithosphere. For the cooling time of oceanic lithosphere, ocean isochrons from Mueller et al. (2008) are used while for Campos continental margin lithosphere, a breakup age of 110 Ma has been used (Torsvik et al., 2009). Sediment densities used within the gravity inversion are assumed to be compaction controlled (Chappell & Kusznir, 2008) and assume a shaly-sand lithology (except for salt).

Fig. 4b shows crustal basement thickness approaches 30 km or more at the coast, which then reduces distally towards the deep ocean in the east. Predicted crustal thicknesses within the oceanic domain range from 5 to 15 km. These larger values may correspond to anomalously thick oceanic crust or, more likely, normal thickness oceanic crust with subsequent superimposed intraplate magmatism. Within the OCT regions, the width of the transition from proximal thick to distal thin crust can be seen to decrease northwards.

As already mentioned, the public domain sediment thickness used to produce the crustal thickness map shown in Fig. 4b has the largest uncertainty. While the crustal thickness map shown made from gravity inversion using public domain sediment thickness gives a useful regional overview, more accurate sediment thickness data would provide a more accurate crustal thickness prediction from gravity inversion.

As a consequence, the seismic profiles shown in Fig. 5 have been used to produce improved sediment thickness for the northern, central and southern profiles. This more accurate sediment thickness has been used in the gravity inversion to produce improved determinations of Moho depth and crustal basement thickness for the three Campos rifted

margin profiles. It is important that the gravity inversion using the more accurate sediment thickness from the seismic profiles is carried out in 3D rather than using 2D modelling. 3D inversion allows for the regional (non 2D) variations in bathymetry and free-air gravity anomaly to be properly incorporated in the gravity inversion and also the 3D long wavelength lithosphere thermal gravity anomaly correction. 2D modelling of individual profiles introduces significant errors and should be avoided where possible. The free-air gravity anomaly data from satellite altimetry is preferred to ship derived gravity data because it is laterally more extensive and, at the longer wavelengths (>50 km) used in the gravity inversion to determine Moho depth, has been shown to be as accurate as ship derived data.

The crustal cross-sections for the three profiles, with Moho from the improved gravity inversion, are shown in Fig. 6a, displaying the distribution of crustal basement thinning across the OCT. The benefits of using sediment thicknesses derived from the seismic reflection data rather than from the global public domain sediment thickness compilation are greater detail and less uncertainty in top basement geometry and an improved Moho depth and crustal basement thickness derived from gravity inversion (cross-sections are compared in supplementary material Fig. S2).

Sensitivity tests of how ocean isochrons (from Mueller et al., 2007) are used to condition the thermal model for the determination of the lithosphere thermal gravity anomaly correction have been carried out. Our preferred gravity inversion model uses an oldest ocean isochron and breakup age of 110 Ma. The sensitivity tests show that using 100 Ma or 120 Ma does not significantly change the Moho depths determined from gravity inversion for the three profiles (sensitivity tests are shown in supplementary material Fig. S3).

The seismic reflection sections show the presence of Aptian salt. Inclusion of the salt horizon (with density 2200 kg/m^3) in the sediment density model used in the gravity inversion makes little difference to Moho depth and crustal basement. This is consistent with what has been previously observed in other salt basins (e.g. Cowie et al., 2015, Steinberg et al., 2018) and is because the salt has often risen to its depth of neutral buoyancy within the sedimentary column whose density increases with depth because of compaction.

The crustal cross-sections shown in Fig. 6a derived from gravity inversion using seismic reflection sediment thicknesses also show differences in OCT structure between the northern, central and southern profiles. The northern profile shows a relatively abrupt oceanwards thinning of the crust while the central and southern profiles show a more gradual decrease. The significance of these different OCT structures will be discussed later.

The seismic sections (Fig. 5) shows some deep reflections which could be interpreted as being from the Moho, however they are discontinuous and indistinct. In order to compare the Moho depths predicted from gravity inversion with the Moho interpretations on the seismic sections, we have converted the Moho depths from gravity inversion into time sections (TWT). The conversion of gravity Moho depth to TWT has been made by converting the thickness of crustal basement from gravity inversion into interval TWT and adding it to the TWT of top basement (which was also used to determine sediment thickness). A seismic velocity of 6530 m/s has been used for crustal basement in the conversion to TWT. This seismic velocity corresponds to the crustal basement density of 2850 kg/m^3 used in the gravity inversion as

predicted by the Nafe-Drake relationship between density and seismic velocity (Ludwig et al., 1970). Fig. 6b shows the comparison of the seismic interpretations of Moho with the predicted TWT of gravity Moho. The comparison is generally good and suggests that the seismic reflection data is able to image Moho in some places. The seismic Moho has a TWT of approximately 10 sec. which is consistent with that generally proposed by Warner (1987).

4. Results – Identification of OCT domains

The crustal architecture of the Campos rifted margin shown on the three profiles (Fig. 5 and 6) displays important variations from south to north. Four major crustal domains have been identified and named as Proximal, Necking zone (NZ), Distal Highly Extended Domain (HED), and Embryonic Oceanic Domains (EOD, for margin nomenclature, see Stanton et al., 2016). Each domain has specific crustal basement thickness (from gravity inversion), magnetic and seismic signatures that characterize its nature and define inter-domain boundaries.

4.1. Regional magnetic and crustal thickness anomalies

From the coast, two high amplitude magnetic anomalies are observed: the Campos and Santos Magnetic Highs (CMH and SMH respectively, Stanton et al., 2010; Stanton and Schmitt, 2015) along the proximal margin of the southern Campos and northern Santos basins (Fig. 3). They exhibit NE-SW trends and are associated with Moho highs (Fig. 5), forming a nearly continuous lineament from Santos to Campos basins, with amplitudes ranging from 200-600 nT. The highs display both short (<10 km) and long wavelength anomalies oriented NNE-SSW (Fig. 3b and c, respectively), which are absent north of 22^{o}S.

The CMH magnetic signature can be correlated with the CFTD anomaly pattern onshore, where short-wavelength, high amplitude anomalies are observed, mainly related to granitoids and Mesozoic dikes (Stanton et al., 2010). Offshore, the CMH is coincident with the location of drilled basalts (Fodor et al., 1983; Mizusaki et al., 1998) (white circles in Fig. 3), assigned as lava flows and dated between 128-122 Ma. Potential field modeling suggests the presence of both shallow and deep mafic igneous sources associated with these highs (Stanton et al., 2010) which is also supported by the upward continuation and the analytic signal of the magnetic anomalies maps (Fig. 3b and d, respectively). A proximal regional lineament is associated with the CMH and SMH, prolongating from the central Santos to Campos basins and displays similarities with the G Anomaly (Rabinowitz and Labreque, 1979) identified to the south of the Rio Grande Fracture Zone, which was associated with volcanic rocks (seaward dipping reflectors).

A distal positive lineament (circa 300 nT) is observed trending N70^{o}E in the southern Campos (white dotted lines in Fig. 3) and NNE in the Central and Northern Campos segment, here named SouthEast Magnetic Anomaly (SEMA). The change in its trend direction is accompanied by an inflexion of the crustal thinning as well (Fig. 4). The proximal and distal magnetic highs trends are all interrupted by a large ENE-WSW oriented negative zone (Fig. 3) that corresponds, on seismic data, to a zone of subvertical normal faults. It shifts right-laterally the positive trends resulting on en echelon pattern, suggesting a tectonic segmentation. Seawards

from the SEMA, high amplitude and short wavelength anomalies characterize a pattern similar to oceanic crust (number 3, Fig. 3). In the northern Campos a conspicuous NW-SE negative trend is observed (black dotted line in Fig. 3), which is aligned with the Vitoria-Colatina Dike Swarm (VCDS) (Aristizábal, 2013, number 4 in Fig. 1). The crustal necking location from the gravity analysis is represented as a blue dotted line in Fig. 3 for comparison with the magnetic pattern.

4.2. Crustal domains

• The proximal domain

The proximal domain of Campos rifted margin exhibits contrasting geophysical signatures between the southern and northern segments (Fig. 3, 5 and 6). On the Southern Campos margin the initial crustal thickness from gravity inversion is circa 35 km (Fig. 6). The Campos Magnetic High (CMH) at the continental shelf coincides with a region of Moho rise (Fig. 5 and 6) and drilled Early Cretaceous basalts (white circles at Fig. 3). The middle and lower crust display high reflective-large-scale folds. A deep and reflective seismic layer is observed between 9 and 10 seconds (Fig. 5), which coincide with the gravity inversion Moho (Fig. 6). As this deep reflectivity is associated with potential field anomalies and superficial basaltic layers, it might indicate magmatic intrusions at depth.

On the Central Campos margin, the upper crust displays a reflection free seismic pattern (Fig. 5), while the middle and lower crust display sub-horizontal high amplitude and concave-up reflectors (see detail in Fig. 7c), with two different genetic set of faults: 1) an upper crust syn-rift fault system, and 2) a middle/lower crust low angle-west dipping reverse fault systems, probably Precambrian (Fig. 7c). As observed on sections S and C, the middle to lower crust is characterized by a highly reflective basement, with a structural pattern similar to the folded nappes observed in the CFTD (Schmitt et al., 2016; Fig. 1).

On the Northern Campos margin the Proximal Domain is narrow (<40 km) and it is not associated with magnetic anomalies (Fig. 3). The initial crustal thickness is circa 35 km (Fig. 6) and has poor basement reflectivity (Fig. 5). Deep crustal reflectors exhibiting dome shape are observed that resemble deep shear zones.

• The necking zone

The crustal Necking Zone (NZ) of a margin is where the extension and crustal thinning localize. The NZ is shown in Fig. 3 as a blue dotted line. On the Southern and Central Campos margins, it is characterized by positive magnetic anomalies (Fig. 3), differing from the Northern Campos margin, where no magnetic anomalies are observed. A gentle and progressive crustal thinning is observed, and middle and lower crust exhibit a series of concave-up reflectors separated by low angle structures (Fig. 5). The upper crust shows syn-rift tilted fault blocks. Section S images a structural high with reflection free pattern at the beginning of the NZ, which coincides with the CMH and drilled basalts, suggesting a volcanic construction (Fig. 7a). Seawards a large structural high (~30 km wide) also displays reflection-free seismic facies similar to igneous bodies (Fig. 7b)) which may indicate that extension was accompanied by magmatism.

On the Central Campos margin crustal thinning (Fig. 5 and 6) is distributed along two main zones, with intracrustal reflectors dipping towards the basin at middle crust (Fig. 7c). A massive texture is observed for the upper crust. Seawards an abrupt basement deepening coincides with deep reflectors rising sharply, leading to extreme crustal thinning in the Distal Highly Extended Domain (HED). Between the Central and Northern Campos margin segments, a marked difference in basement texture is observed, as shown in detail at Fig. 8b. On the Northern Campos margin the upper crust shows a homogeneous pattern (Fig. 5), the top basement deepens steeply leading to a rapid crustal thinning and localization of the deformation. It displays highly reflective horizons at depth that correlates with a subtle rise of the Moho predicted from gravity inversion. The crustal thickness map indicates a northwards crustal thinning axis towards this area (Fig. 4) of the Campos margin.

- The distal highly extended domain (HED)

On the Southern Campos margin the HED is located seawards of a volcanic high (fig. 5) and crustal thickness decreases to circa 9 km (Fig. 6). It is characterized by a magnetic low (Fig. 3), suggesting an absence of magmatism. A regional negative lineament trending NE-SW (marked by a zone of negative value to the north of SEMA) corresponds on the seismic data to a sub-vertical fault zone dipping to NE, representing a crustal discontinuity. Seawards the magnetic pattern displays short wavelength lineaments, similar to oceanic crust (anomaly 3 in Fig.3). The basement and sub-salt sequence are poorly imaged due to the thick salt layers. On Section S, the COB is not imaged and the oceanic domain lies within an area of post rift magmatic activity.

The Central Campos margin is characterized by large continentward tilted blocks, filled with thick syn-rift sequences (Fig. 5) and no associated magnetic anomalies (Fig. 3). The COB corresponds to an outer high overlain by allochthonous salt, displaying increasing magnetic anomalies seawards. A thin oceanic crust is observed and shows two-layers with an upper layer displaying faults dipping downwards to the ocean (Fig. 8b). It evolves seawards into normal thickness oceanic crust.

On the Northern Campos margin (Fig. 5 and 6), the HED is circa 120 km wide and displays tilted blocks covered by thick syn-rift sequences. The COB is represented by an outer high onto which the first oceanic crust abuts with normal thickness. The overlying allochthonous salt-tongues end abruptly. A magnetic high marks the COB, and magnetic lineaments trends inflect seawards to NNE (Fig. 3) suggesting a transition to the oceanic domain.

5. Discussion

5.1. The role of basement inheritance on Campos rifted margin architecture

The Campos rifted margin (CRM) shows marked differences in key architectural elements from south to north, which correlates with changes in crustal composition, age, structure and magmatic activity, as shown in Fig. 9 and 10.

The proximal and necking zones display variations along strike in magnetic anomalies and syn-rift magmatic rocks abundance, especially at the Southern and Central segments which exhibit important magmatic activity evidenced also from seismic data and deep wells that perforate syn-rift volcanic rocks. On the contrary, no first-order magnetic anomalies or magmatic rocks are observed in the Northern segment.

The necking zone is widest at Central Campos margin and narrows northwards (Fig. 9 and 10), where abrupt necking of the crust contrasts with the Central and Southern Campos segments gradual thinning. The wider necking zone resulted in larger (i.e. wider) accommodation space and more extensive syn-rift deposits, as documented by Dias et al. (1987). Interestingly, the Central segment is characterized by less magmatism when compared to the Southern segment, as shown by the analytic signal map of Fig. 3d and supported by fewer basalts from wells. These evidences, along with the high ductile versus brittle ratio inferred from the seismic pattern (Fig. 5), may have favored the crustal extension during the early rift stage.

On the Central and Southern Campos margins, the crust seems to be bipartite from the seismic point of view, displaying an upper reflection-free (or massive) crust above a highly reflective and layered middle/lower crust, with concave-up reflectors and low angle structures. These structures are similar to the onshore nappes and thrusts dipping to the NW at the adjacent Neoproterozoic supracrustal sequence of the CFTD, interleaved with the high strain domains of the Paleoproterozoic basement (Fig. 7a and c). The more massive/homogeneous upper crust could represent the low strain domains of that basement, without penetrative foliation. This is supported by recent drilling at the Cabo Frio High that revealed CFTD Paleoproterozoic orthogneisses with U-Pb age on igneous zircons of 1980 +-18 Ma (Carmo et al., 2017).

All these units are structurally and compositionally distinct from the northern and northeastern basements of the Neoproterozoic/Cambrian mobile belts of Ribeira (Oriental Terrane) and Araçuaí (as discussed above in item 2.1 – Fig. 10), as evidenced by geological (Heilbron et al., 2004; Schmitt et al., 2008) and geophysical data (Figueiredo et al., 2008; Assunção et al., 2006). From these observations and the drilling results (Carmo et al., 2017), we interpret the crust on the Southern and Central Campos margin to be an offshore extension of the onshore CFTD.

On the Northern Campos segment our observations from seismic data suggest the presence of a more massive crystalline basement at the Proximal and Necking zones, with deep shear zones, when compared to the central and southern segments (Fig. 8). The transition between these and the northern Campos segments is associated with an important variation in crustal thickness and seismic texture (Fig. 8), suggesting the existence of a crustal discontinuity. This discontinuity coincides with a change in orientation of the mantle anisotropy onshore, that inflects from NE-SW to NW-SE (Assunção et al., 2006 – Fig. 10) at the transition between the Ribeira Belt (Oriental Terrane) and the Araçuaí Belt (blue dashed line in Fig. 10). Offshore this region agrees with the possible continuation of the Cabo Frio Tectonic Domain towards NE. Until now there is no additional data to constrain the exact boundaries of these terranes offshore. In an attempt to extend offshore the tectonic contacts/terranes based on the previous geological and geophysical observations, we propose that: 1) the northern Campos Basin basement could correspond to the Aracuaí belt; and 2) the CFTD seems to correspond to

the central and southern segments basement (Fig. 10). From the geological point of view, the Araçuaí Belt shows a very distinctive framework in comparison with the CFTD, as represented in the comparative geological sections of Fig. 10, in part controlled by its composition, what would explain the distinct nature of the basement on the northern Campos (Fig. 5 and 8). The major Cambro-Ordovician magmatic intrusions related to the post-collisional stage, may have obliterated most of the original orogenic structures, configuring a more homogenous and less foliated crust (Degler et al., 2016; De Campos et al., 2016). In addition, the Araçuaí Belt displays larger volumes of basic rocks in comparison with the predominant acidic/intermediate rocks of the Ribeira Belt (Oriental terrane – De Campos et al., 2016). This characteristic may have exerted a control during rifting, since the crust would have been more competent, localizing the strain and resulting on the observed abrupt thinning and narrow margin architecture (Fig. 8b, 9 and 10).

5.2. Structural evolution: from early rifting to breakup stages

The margin architecture reflects the lithosphere response to extension, which is dependent on its strength and thermal state. A broad region of thinning suggests a distributed deformation, resulting in a wider margin, and vice versa. On the northern Campos margin, the crust and mantle deformation couple at the NZ and are accommodated by upper crust faults and shear zones near the base of the crust. On the central and southern Campos margins, the extension is accommodated by widely distributed middle and lower crust ductile structures, which are possibly shear zones. Large-scale grabens seem to be controlled by a SE dipping *decollement* at the brittle-ductile transition, (Fig. 8b), suggesting a depth-dependent extension. It is possible that this decollement may have been favored by the pre-existing contacts between the layered crust of CFTD, represented by its Paleoproterozoic and the Neoproterozoic units (Fig. 7a). The observed high ratio of ductile relative to brittle crustal layers (Fig. 9) indicates that the crust was less resistant to deformation, allowing the development of a wide decoupled zone, as has been demonstrated by modeling (Corti et al., 2010; Capelleti et al., 2013; Brune et al., 2016).

These basement heterogeneities would have also affected the rift propagation from south to north, localizing the extension where more foliated lithologies were present and deviating it around more resistant or “locked” areas (Wijk et al., 2004). This would favor margin segmentation, forming articulated basins within areas of “strong” rheology, and deeper basins at “weak” rheology (Capelleti et al., 2013). It would also influence the development of accommodation space, as observed at the Central Campos Rifted Margin (CRM). We propose that CRM deformation was dominated by the pre-existing basement inheritance in the early stages, similar to that observed at the Barents Sea basins, where reactivation of the deep structure controlled the present-day geometries of basins (Gernigon et al., 2014). Nevertheless, the Distal Highly-extended Domain (HED) forms a uniformly wide region along the CRM, with the breakup only being achieved after considerable crustal extension (Fig. 10)., Variations in margin width seem to result primarily from differences in thinning geometry created in the early rifting stages and are dependent on the preexisting basement composition and structure, as represented in Fig. 10. However, once the crust is highly extended, inheritance seems to exert less control on the deformation, favoring a more uniform extension, which is also supported by recent lithosphere numerical modeling (Manatschal et al., 2015).

5.3 Architectural styles of the Campos rifted margin

We have identified three main Architectural types at Campos Rifted Margin, represented in Fig. 9:

a) **Type 1** (Northern Campos, section N in Fig. 5) is characterized by an abrupt architecture, with a narrow and steep crustal necking zone. The crust is affected by few superficial faults and basal shear zones. The HED is wide and devoid of magmatism (Fig. 3d) and ends at an outer high with a volcanic COB, followed by normal thickness oceanic crust.

b) **Type 2** (Central Campos, section C in Fig. 5) is characterized by a layered crust, a relative high ratio of ductile versus brittle crustal layers, resulting in a wide crustal necking zone accommodated by faults in the upper crust, a regional decollement at the brittle/ductile transition and deep ductile shear zones, and localized magmatism. A wide HED displays domino-style extensional fault blocks continentward and an outer high with minor volcanism at the COB (Fig. 3d), followed by thin embryonic oceanic crust;

c) **Type 3** (Southern Campos, section C in Fig. 5) displays a layered crust and gradual NZ, similar to Type 2 but is more affected by magmatism (Fig. 3d). The HED is wide and devoid of magmatism.

These three crustal types are associated with large differences in their sedimentary sequences, evidencing that these exerted control on the sedimentation. In Type 1 at Northern Campos, the syn-rift sequence along the inner margin is thin or absent, indicating that the crust was resistant to extension during initial rifting. The syn-rift sequence is present in Type 3, but it exhibits the greatest thickness in Type 2, at Central Campos (Fig. 8). This evidence suggests that the crust at the Central Campos margin underwent greater extension, which may be related to a high ductile/brittle ratio. According to Capelleti et al. (2013), in weak lower crust, the deformation is concentrated at the inner margin in the initial stages of rifting, developing thick syn-rift sequences. In contrast, a strong lower crust would result in domino-style extensional faulting and basins, with a thinner syn-rift package, as observed in Type 1 at the northern Campos margin. A possible higher geothermal gradient suggested by the greater amount of magmatic rocks at the Southern Campos margin (Type 3) would result in initial basement uplift, counter-balancing the subsidence due to crustal thinning and reducing the initial accommodation space.

6. Conclusions

We present evidence for the inter-relation between basement inheritance, magmatism and rift evolution on Campos Rifted Margin controlling the present day margin architecture, as summarized below.

1. The Campos margin shows a clear variation in ocean-continent transition (OCT) structure from north to south. In the north the margin shows a narrow necking zone while in the central and southern sections it shows a broader necking zone. A wide highly extended domain (HED) is observed throughout this entire segment of the Brazilian margin.

2. This variation from north to south in OCT structure correlates with variations in pre-rift basement heterogeneities observed onshore from surface geology. The presence of heterogeneous (layered) crust of the CFTD at southern and central Campos margin or a more homogeneous crust of the Aracuaí Belt to the north determined the localization of the deformation and segmentation and the variation of the depositional space.

3. The optimal conditions for sedimentary basin formation seem to be associated with an inherited basement characterized by preexisting structures, a layered crust with a high ductile versus brittle ratio (enabling a widely distributed deformation), and low syn-rift magmatism (normal geotherm favoring the syn-rift subsidence).

4. The thinning geometry seems to be a first-order parameter in defining the margin architecture and is determined by pre-rift conditions and magma budget. However, when the crust is highly extended, it favors a more “uniform¨ deformation, creating a regional sag basin and nearly synchronous breakup.

Acknowledgements

The authors are grateful to CAPES “Science Without Borders” Program for Natasha Stanton Young Talent Grant. This paper is a contribution to IGCP-628 “The geological map and tectonic evolution of Gondwana”.

References

Aristizábal, C.I.O., 2013. Tectônica Mesozoica do Enxame de Diques Vitória-Ecoporanga e do Alto Estrutural de Vitória (ES), PhD thesis, Universidade Federal Fluminense (unpublished).

Alvey, A., Gaina, C., Kusznir, N.J., Torsvik, T.H., 2008. Integrated crustal thickness mapping and plate reconstructions for the high Arctic, Earth planet. Sci. Lett. 274, 310–321. https://doi.org/10.1016/j.epsl.2008.07.036.

Allemand, P., Brun, J.P., 1991. Width of continental rifts and rheological layering of the lithosphere. Tectonophysics. 188, 63–69. https://doi.org/10.1016/0040-1951(91)90314-I.

Assumpção, M., James, D., Snoke A., 2002. Crustal Thickness in SE Brazilian Shield by receiver function analysis: Implications for isostatic compensation. J. Geophys. Res. 107, 1-14. https://doi.org/10.1029/2001JB000422.

Assumpção, M., Heintz, M., Vauchez, A., Egydio-Silva, M., 2006. Upper mantle anisotropy in SE and central Brazil from SKS splitting: Evidence of asthenospheric flow around a cratonic keel: Earth planet. Sci. Lett. 250, 224–240. https://doi.org/10.1016/j.epsl.2006.07.038.

Brune, S., Heine, C., Clift, P. D., Pérez-Gussinyé, M., 2017. Rifted margin architecture and crustal rheology: Reviewing Iberia-Newfoundland, Central South Atlantic, and South China Sea. Mar. Petrol. Geol. 79, 257-281. https://doi.org/10.1016/j.marpetgeo.2016.10.018.

Buck, W.R., 1991. Modes of continental lithospheric extension. J. Geophys. Res. 96, 20161–20178. https://doi.org/10.1029/91JB01485.

Callot, J.P., Geoffroy, L., Brun, J.P., 2002. Development of volcanic passive margins: Three-dimensional laboratory models. Tectonics. 21, 1052. http://doi:10.1029/2001TC901019.

Cappelletti, A., Tsikalas, F., Nestola, Y., Cavozzi, C., Argnani, A., Meda, M., Salvi, F., 2013. Impact of lithospheric heterogeneities on continental rifting evolution: constraints from analogue modelling on South Atlantic margins. Tectonophysics. 608, 30-50. https://dx.doi.org/10.1016/j.tecto.2013.09.026.

Carvas, K.Z., 2016. Diques mesozoicos subalcalinos de baixo titanio da região dos Lagos (RJ): geoquímica e geocronologia 40Ar/39Ar. MSc. thesis. Universidade de São Paulo.

Chang, H.K., Kowsmann, R.O., Figueiredo, A.M.F., Bender, A.A., 1992. Tectonics and stratigraphy of the East Brazil Rift system: an overview, In: P.A. Ziegler (Eds), Geodynamics of Rifting, volume II. Case History Studies on Rifts: North and South America and Africa. Tectonophysics. 213, 97-138.

Chappell, A.R., Kusznir, N.J., 2008. Three-dimensional gravity inversion for Moho depth at rifted continental margins incorporating a lithosphere thermal gravity anomaly correction, Geophys. J. Int. 174.1–13. https://doi.org/10.1111/j.1365-246X.2008.03803.x.

Chenin, P., Manatschal, G., Lavier, L., Erratt, D., 2015. Assessing the impact of orogenic inheritance on the architecture, timing and magmatic budget of the North Atlantic rift system: a mapping approach. J. Geol. Soc. L. https://doi:10.1144/jgs2014-139.

Corti, G., Ranalli, G., Mulugeta, G., Agostini, A., Sani, F., Zugu, A., 2010. Control of the rheological structure of the lithosphere on the inward migration of tectonic activity during continental rifting. Tectonophysics. 490, 165-172. https://doi.org/10.1016/j.tecto.2010.05.004.

Corval, A., 2005. Petrogênese das suítes basálticas toleíticas do Enxame de Diques da Serra do Mar nos setores central e norte do Estado do Rio de Janeiro. Msc thesis, UERJ.

Cowie, L., Kusznir, N., Manatschal, G., 2015. Determining the COB location along the Iberian margin and Galicia Bank from gravity anomaly inversion, residual depth anomaly and subsidence analysis. Geophys. J. Intern. 203, 1355-1372. https://doi:10.1093/gji/ggv367.

Cowie, L. Angelo, R. M., Kusznir, N. J., Manatschal, G., Horn, B., 2015. The palaeo-bathymetry of base Aptian salt deposition on the northern Angolan rifted margin: constraints from flexural back-stripping and reverse post-break-up thermal subsidence modelling. Petrol. Geosc. https://doi:10.1144/petgeo2014-087.

De Campos, C. Medeiros, S., Mendes, J., Pedrosa-Soares, A.C., Dussin, I., Ludka, I., Dantas, E., 2016. Cambro-Ordovician Magmatism in the Araçuaí Belt (SE Brazil): snapshots from a post-collisional event. J. S. Am. Earth Sci. http://dx.doi.org/10.1016/j.jsames.2015.11.016.

Deckart, K., Feraud, G., Marques, L.S., Bertrand, H., 1998. New time constraints on dyke swarms related to the Parana & Etendeka magmatic province, and subsequent South Atlantic opening, southeastern Brazil. J. Volcan. Geotherm. Res. 80, 67-83. https://doi.org/10.1016/S0377-0273(97)00038-3.

Degler, R., Pedrosa-Soares, A., Dussin, I., Queiroga, G., Schulz, B., 2017. Contrasting provenance and timing of metamorphism from paragneisses of the Araçuaí-Ribeira orogenic system, Brazil: Hints for Western Gondwana assembly. Gond. Res. 51, 30-50. https://doi.org/10.1016/j.gr.2017.07.004.

Divins, D.L., 2003. Total Sediment Thickness of the World's Oceans & Marginal Seas. NOAA National Geophysical Data Center, Boulder, CO.

Dunbar, J. A., Sawyer, D.S., 1989. How preexisting weaknesses control the style of continental breakup. J. Geophys. Res. 94, 7278–7292. https://doi.org/ 10.1029/JB094iB06p07278.

Duretz, T., Petri, B., Mohn, G., Schmalholz, S.M., Schenker, F.L., Müntener, O., 2016. The importance of structural softening for the evolution and architecture of passive margins. Sci. Rep. 6, 38704. https://doi.org/10.1038/srep38704.

Fodor, R.V., Vetter, S.K., 1984. Rift-zone magmatism: petrology of basaltic rocks transitional from CFB to MORB, southeastern Brazil margin. Contrib. Mineral. Petrol. 88, 307,984. https://doi.org/10.1007/BF00376755.

Figueiredo, I., Meju, M.A., Fontes, S.L., 2008. Heterogeneous crust and upper mantle across the SE Brazilian Highlands and the relationship to surface deformation as inferred from magnetotelluric imaging. J. Geophys. Res. 113, B03404. https://doi.org/ 10.1029/2007JB005108.

Gernigon, L. Ringenbach, J.C., Planke, S., Le Gall, B., 2004. Deep structures and breakup along volcanic rifted margins: insights from integrated studies along the outer Vøring Basin (Norway). Mar. Petrol. Geol. 21 (3), 363-372. https://doi:10.1016/j.marpetgeo.2004.01.005.

Gernigon, L., Brönner, M., Roberts, D., Olesen, O., Nasuti, N., Yamasaki., T., 2014. Crustal and basin evolution of the southwestern Barents Sea: from Caledonian orogeny to continental breakup. Tectonics. 33 , 347-373. https://dx.doi.org/10.1002/2013TC003439.

Guardado, L.R., Gamboa, L.A.P., Lucchesi, C.F., 1989. Petroleum geology of the Campos Basin, Brazil, a model for a producing Atlantic type Basin, In: Edwards, J. D., Santogrossi P.A. (eds); Divergent/passive margin basins. American Association of Petroleum Geologist Memoir 48, 3–79. https://doi.org/10.1306/M48508C1.

Guedes E., Heilbron M., Vasconcelos P.M., Valeriano, C.M., Almeida J.C.H., Teixeira W., Thomaz Filho A., 2005. K/Ar and 40Ar/39Ar ages of dykes emplaced in the on-shore basement of the Santos Basin, Resende area, SE Brazil: implications for the south Atlantic opening and Tertiary reactivation. J. S. Am. Earth Sci. 18, 371-182. https://doi.org/ 10.1016/j.jsames.2004.11.008.

Duretz, T. Petri, B., Mohn, G., Schmalholz, S.M., Schenker, F.L., Müntener, O., 2016. The importance of structural softening for the evolution and architecture of passive margins. Scientific Reports 6. e38704. https://doi.org/10.1038/srep38704.

Heilbron, M., Pedrosa-Soares, A.C., Campos Neto, M.C., Silva, L.C., Trouw, R.A.J., Janasi, V.A., 2004. Província Mantiqueira, in: Mantessoneto, V., Bartorelli, A., Carneiro, C.D.R., Brito-

Neves, B.B. (Eds.), Geologia do Continente Sul Americano: Evolução da Obra de Fernando Flavio Marques de Almeida. Cap XIII, pp. 203-235.

Heine, C., Zoethout, J., Müller, R.D., 2013. Kinematics of South Atlantic rift. Solid Earth. 4, 215-253. https://doi.org/10.5194/se-4-215-2013.

Huismans, R.S. Beaumont, C., 2011. Depth-dependent extension, two-stage breakup and cratonic underplating at rifted margins. Nature. 473. https://doi.org/10.1038/nature09988.

Kusznir, N. J., Park, R.G., 1987. The extensional strength of the continental lithosphere: its dependence on geothermal gradient, and crustal composition and thickness. Geol. Soc. Lond. Spec. Publ. 28 , 35–52. https://doi.org/10.1144/GSL.SP.1987.028.01.04.

Lobo, J., 2007. Petrogênese dos Basaltos do Eocretáceo das Bacias de Campos e Pelotas e Implicações na Geodinâmica do Rifteamento do Gondwana Ocidental. Universidade do Estado do Rio de Janeiro, PhD thesis.

Marzoli, A., Melluso, L., Morra, V., Renne, P.R., Sgrosso, I., D'Antonio, M., Duarte Morais, L., Morais, E.A.A., Ricci, G., 1999. Geochronology and petrology of Cretaceous basaltic magmatism in the Kwanza basin (western Angola), and relationships with the Paraná-Etendeka continental flood basalt province. J. Geodyn. 28 (4–5), 341–356. https://dx.doi.org/10.1016/S0264-3707 (99)00014-9.

Miller, H.G., Singh, V., 1994. Potential-field tilt - a new concept for location of potential-field sources. J. App. Geophys. 32, 213-217. https://doi.org/10.1016/0926-9851(94)90022-1.

Mizusaki, A.M.P.; Thomaz-Filho, A.; Valença, J., 1988. Volcano-sedimentar sequence of Neocomiam age in Campos Basin (Brazil) Rev. Bras. Geoc., 18 (3), 247-251.

Mizusaki, A.M.P., Petriniz, R., Bellieni, G., Comin-Chiaramonti, P., Dias, J., De Min, A., Piccirillo, E.M., 1992. Basalt magmatism along the passive continental margin of SE Brazil (Campos Basin). Contrib. Mineral Petrol. 111, 143-160.

Mohriak, W.U., Mello, M.R., Dewey, J.F., Maxwell, J.R., 1990. Petroleum geology of the Campos Basin, offshore Brazil. Geol. Soc. Lond. Spec. Publ. 50 (1), 119–141. https://dx.doi.org/10.1144/GSL.SP.1990.050.01.07.

Müller, R.D., Sdrolias, M., Gaina, C., Roest, W.R., 2008. Age, spreading rates and spreading symmetry of the world's ocean crust. Geochem. Geophys. Geosyst. 9, Q04006. https://doi.org/10.1029/2007GC001743.

Oreiro, S.G., Cupertino, J.A., Szatmari, P., Thomaz Filho, A., 2008. Influence of pre-salt alignments in post-Aptian magmatism in the Cabo Frio High and its surrounding, Santos and Campos basins, SE Brazil: an example of non-plume related magmatism. J. S. Am. Earth Sci. 25, 116-131. https:/doi.org/10.1016/j.jsames.2007.08.006 .

Pedrosa-Soares, A.C., Noce, C.M., Wiedemann, C.M., Pinto, C.P., 2001. The Araçuaí–West Congo orogen in Brazil: an overview of a confined orogen formed during Gondwanaland assembly. Precam. Res. 110, 307–323. https://doi.org/10.1016/S0301-9268(01)00174-7.

Torsvik, T.H., Rousse, S., Labails, C. and Smethurst, M.A., 2009. A new scheme for the opening of the South Atlantic Ocean and the dissection of an Aptian salt basin. Geophysical Journal International. 177: 1315-1333. https://doi.org/10.1111/j.1365-246X.2009.04137.x.

Quesnel, Y., Catalán, M., Ishihara, T. 2009. A new global marine magnetic anomaly data set, J. Geophys. Res. 114, B04106. https://doi.org/10.1029/2008JB006144.

Rabinowitz, P.D., LaBrecque, J., 1979. The mesozoic South Atlantic ocean and evolution of its continental margin. J. Geophys. Res. Solid Earth. 84, 5973-6002. https://doi.org/10.1029/JB084iB11p05973.

Sandwell, D.T., Smith, W.H.F., 2009. Global marine gravity from retracked Geosat and ERS-1 altimetry: ridge segmentation versus spreading rate. J Geophys Res. 114, B01411. https://doi.org/10. 1029/2008JB006008.

Savastano, V.L.M., Schmitt, R.S., Araújo, M.N.C., Inocencio, L.C., 2017. Rift brittle deformation of SE-Brazilian continental margin: kinematic analysis of onshore structures relative to the transfer and accommodation zones of southern Campos Basin. J. Struct. Geol. 94, 136-153. http://dx.doi.org/10.1016/j.jsg.2016.11.012.

Schmitt, R.S. Trouw, R.A.J., Van Schmus, W.R., Passchier, C.W., 2008. Cambrian orogeny in the Ribeira Belt (SE Brazil) and correlations within West Gondwana: ties that bind underwater, in: Pankhurst, R.J., Trouw R.A.J., Brioto Neves B.B., De Wit M.J. (eds.) West Gondwana: Pre-Cenozoic Correlations across the South Atlantic Region. Geol. Soc. London, Spec. Pub. 294, 279-296. https://doi.org/10.1144/SP294.15.

Schmitt, R.S., Trouw, R.A.J., Van Schmus, W.R., Pimentel, M.M., 2004. Late amalgamation in the central part of West Gondwana: new geochronological data and the characterization of a Cambrian collisional orogeny in the Ribeira Belt (SE Brazil). Precam. Res. 133, 29-61. https://doi.org/10.1016/j.precamres.2004.03.010.

Schmitt, R.S., Trouw, R.A.J., Schmus, W.R., Armstrong, R., Stanton, N.S.G., 2016. The tectonic significance of the Cabo Frio Tectonic Domain in the SE Brazilian margin: a Paleoproterozoic through Cretaceous saga of a reworked continental margin. Braz. J. Geol. 46, 37-66. https://doi.org/10.1590/2317-4889201620150025.

Schmitt, R.S., Silva, E.A., Collins, A.S., Reeves, C., Fragoso, R.A., Richetti, P.C., Fernandes, G.L. de F., Benedek, M.R., Costa, R.L., Assis, A.P., 2016 Gondwana tectonic evolution recounted through the Gondwana map – IGCP- 628, in: Abstracts 35th Inter. Geol. Cong., Cape Town, Cape Town.

Siedner, G., Mitchel, J.G., 1976. Episodic Mesozoic volcanism in Namibia and Brazil: A K—Ar Isochron study bearing on the opening of the South Atlantic. Earth Planet. Sci. Let. 30, 2, 292-302. https://doi.org/10.1016/0012-821X(76)90256-9.

Stanton, N., Schmitt, R.S., Galdeano, A., Maia, M., Mane, M., 2010. Crustal Structure of the Southeastern Brazilian Margin, Campos Basin, from Aeromagnetic Data: New kinematic constraints. Tectonophysics. 490, 15-27. https://doi.org/10.1016/j.tecto.2010.04.008.

Stanton, N., Schmitt, R., 2015. Onshore-offshore prolongation of structures between Campos and Santos Basins from aeromagnetic data. The 14th International Congress of the Brazilian Geophysical Society, Exp. Abs.

Stanton, N., Manatschal, G., Autin, J., Sauter, D., Maia, M., Viana, A., 2016. Geophysical fingerprints of hyper-extended, exhumed and embryonic oceanic domains: the example from the Iberia–Newfoundland rifted margins. Mar. Geophys. Res. 37, 185. https://doi.org/10.1007/s11001-016-9277-0.

Steinberg, J., Roberts, A.M., Kusznir, N.J., Schafer, K., Karcz, Z., 2018. Crustal structure and post-rift evolution of the Levant Basin. Mar. Petrol. Geol. https://doi.org/10.1016/j.marpetgeo.2018.05.006.

Sutra, E., Manatschal, G., 2012. How does the continental crust thin in a hyperextended rifted Margin? Insights from the Iberia margin. Geology. 40 (2), 139–142. https://dx.doi.org/10.1130/G32786.1.

Tommasi, A., Vauchez, A., 2001. Continental rifting parallel to ancient collisional belts: an effect of the mechanical anisotropy of the lithospheric mantle. Earth Planet. Sci. Let. 185, 199-210. https://doi.org./10.1016/S0012-821X(00)00350-2.

Valente, S.C., Corval, A., Duarte, B.P., Ellam, R.M., Fallick, A.E., Meighan, I.G., Dutra, T., 2007. Tectonic boundaries, crustal weakness zones and plume-subcontinental lithospheric mantle interactions in the Serra do Mar dyke swarm, SE Brazil. Rev. Bras. Geoc. 3, 194-201.

Van Wijk, J.W., Blackman, D.K., 2005. Dynamics of continental rift propagation: the end-member modes. Earth Plan. Sci. Let. 229, 247-258. https://doi.org/10.1016/j.epsl.2004.10.039.

Van Wijk, J.W., van der Meer, R., Cloetingh, S.A.P.L. 2004. Crustal thickening in an extensional regime: application to the mid-Norwegian Vøring margin, Tectonop. 387 (1–4): 217-228, https://doi.org/10.1016/j.tecto.2004.07.049.

Winter, W.R., Jahnert, R.J., França, A.B., 2007. Bacia de Campos, in: Milani, E. J. (eds.); Rangel, H.D.; Bueno, G.V.; Stica, J.M.; Winter, W.R.; Caixeta, J.M.; Pessoa Neto, O.C. Cartas Estratigráficas. Bol. Geoc. Petrobras, Rio de Janeiro. 15, 511-529.

Whitmarsh, R. B., Manatschal, G., 2012. Evolution of magma poor continental margins: from rifting to the onset of seafloor spreading. In, Roberts, D.G. and Bally, A.W. (eds.) Regional Geology and Tectonics: Phanerozoic Passive Margins, Cratonic Basins and Global Tectonic Maps, Vol. 1C. Amsterdam, NL. Elsevier, 327-341. https://doi:10.1016/B978-0-444-56357-6.00008-1.

Yamasaki, T., Gernigon, L., 2009. Styles of lithospheric extension controlled by underplated mafic bodies, Tectonophysics. 468, 169-184. https://doi: 10.1016/j.tecto.2008.04.024.

Zalán, P.V., Severino, M., do, C.G., Rigoti, C.A., Magnavita, L.P., Oliveira, J.A.B., Vianna, A.R., 2011. An Entirely New 3D-view of the Crustal and Mantle Structure of a South Atlantic Passive Margin-Santos, in: Americal Association of Petroleum Geology, Annual Convention and Exhibition. Campos and Espírito Santo basins, Brazil.

Zindler, A., Hart, S., 1986. Chemical Geodynamics. Annual Review of Earth and Planetary Sciences 14: 493-571. https://doi.org/10.1146/annurev.ea.14.050186.002425.

Figure 1

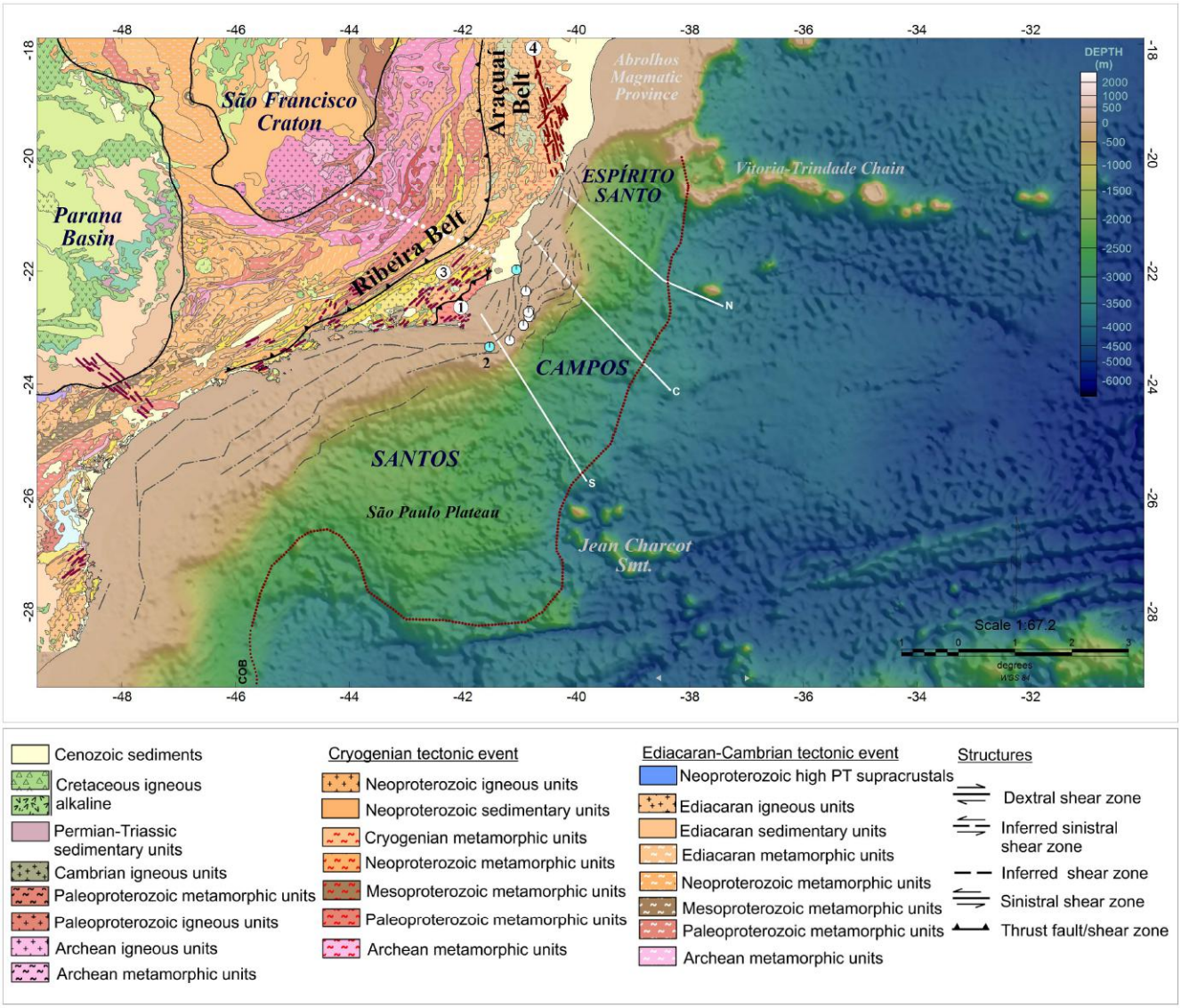

Fig. 1. Geological and tectonic map of Southeastern Brazilian margin (after Schmitt et al., 2004). Onshore geology from Schmitt et al. (2018). 1 - Cabo Frio tectonic Domain (CFTD); 2 - Cabo Frio High; 3 and 4 - dike swarms (represented by red lines): Serra do Mar (after Lobo et al., 2007) and Vitoria-Colatina (Ariztizábal, 2013), respectively. White dashed line – the location of change in direction of mantle anisotropy. Offshore structures after Stanton et al. (2010) and Continent-Ocean Boundary (COB) location from Zalán et al. (2011). White circles- wells that recovered basalts; cyan circles- wells that reached the CFTD basement.

Figure 2

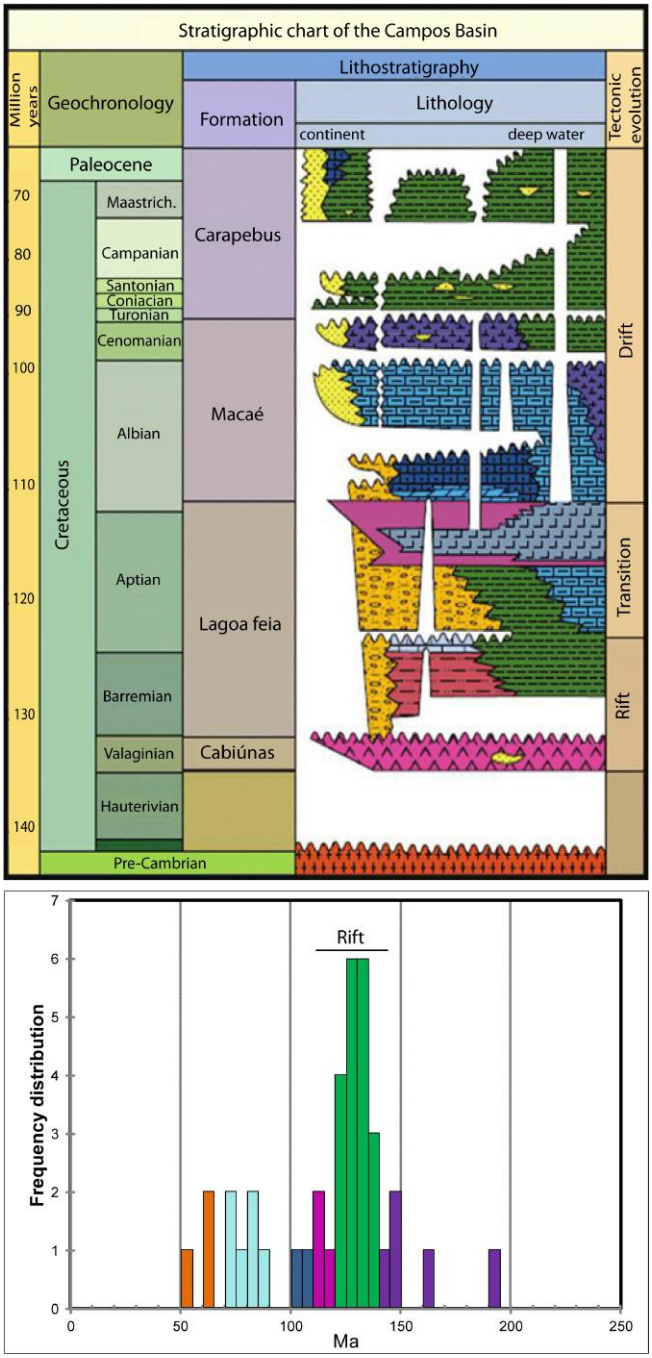

Fig. 2. Simplified stratigraphic chart of Campos Basin (modified from Lourenço et al., 2014, after Winter et al., 2007). A compilation of onshore and offshore Campos Magmatic events is shown below (see text for details).

Figure 3

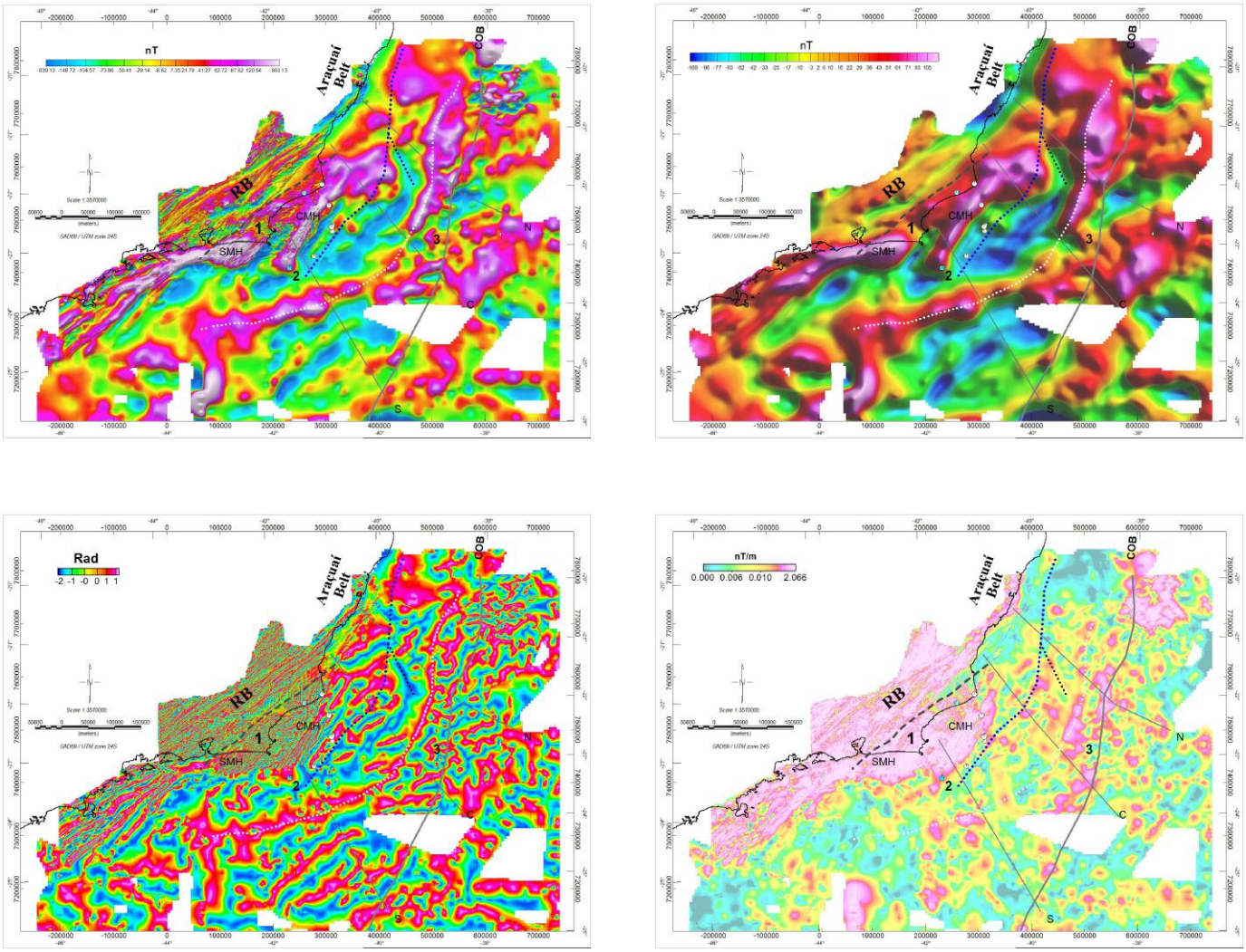

Fig. 3. a) Total magnetic anomaly map; b) Upward continuation of the magnetic anomalies to 10 km height; c) Tilt derivative of the magnetic anomalies; d) Analytic signal of the magnetic anomalies. CMH, SMH - Campos and Santos Magnetic High, respectively; white circles - wells that recovered basalts; cyan circles - wells that reached the CFTD basement; grey lines - seismic cross sections of Fig. 5; dotted lines: white - the South East Magnetic Anomaly (SEMA), black - NW-SE discontinuity, blue - necking zone from gravity.

Figure 4

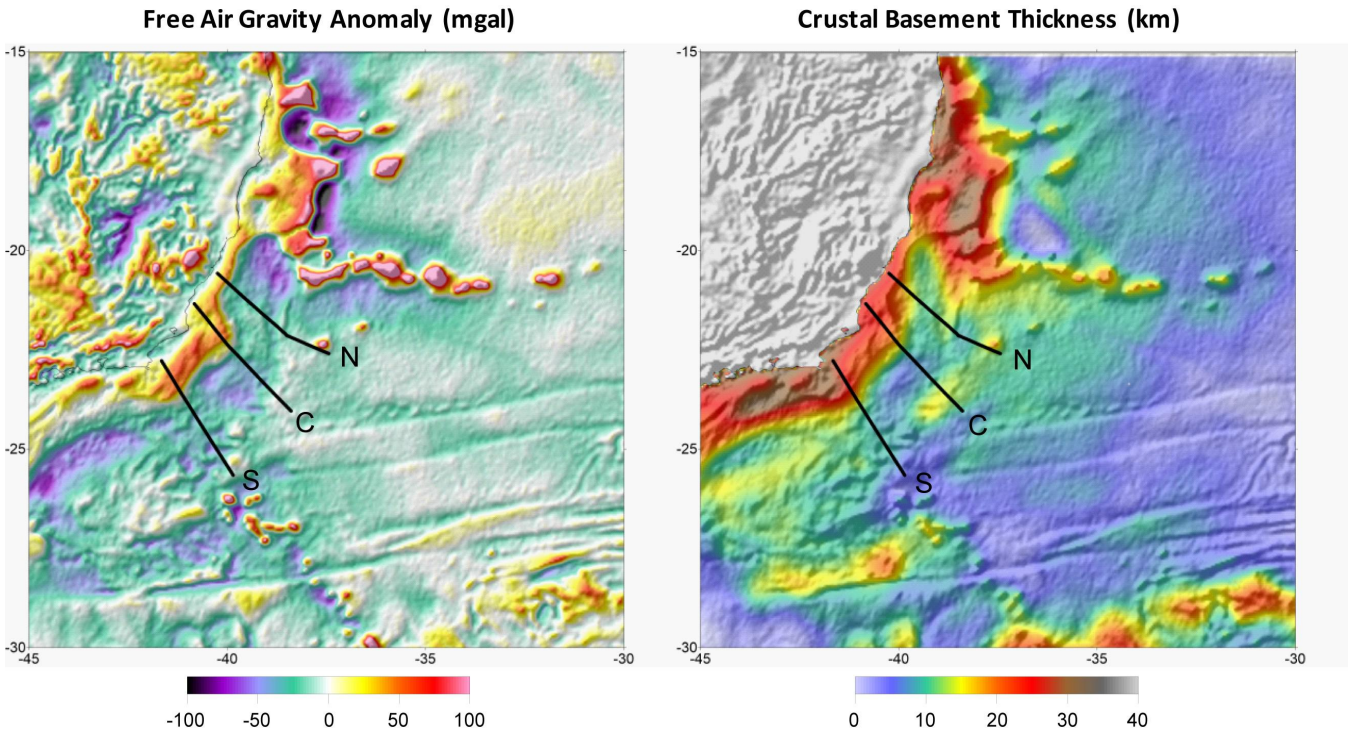

Fig. 4. (a) Free-air gravity anomaly for Campos margin and adjacent areas. (b) Crustal basement thickness derived from gravity inversion using public domain sediment thickness data. The location of profiles (N, C and S) across the Campos margin are shown.

Figure 5a

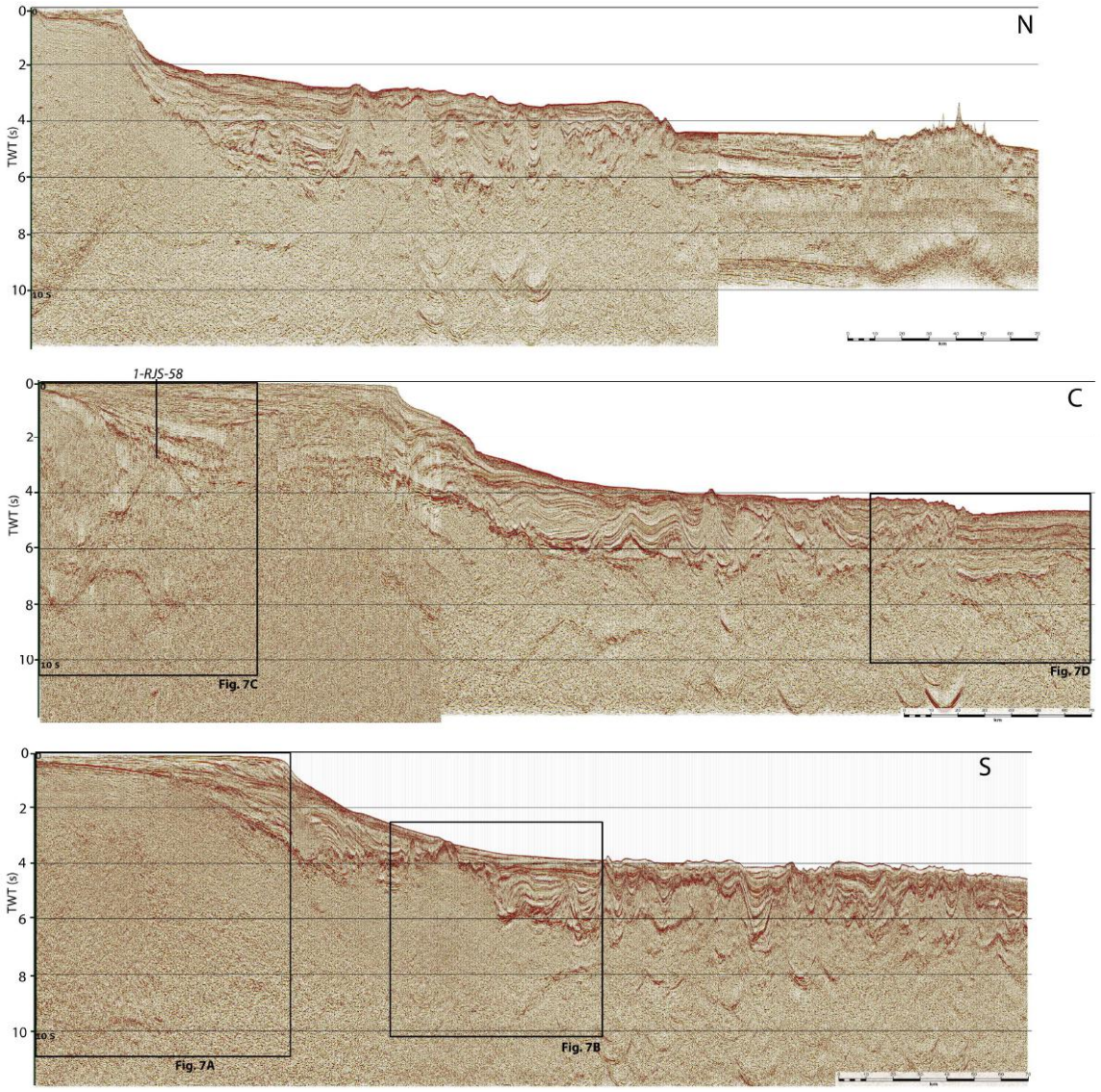

Fig. 5. Seismic cross sections. (a) uninterpreted, showing the location of Fig. 7a-d and 8a-b (black rectangles); and (b) with interpretation, showing the magnetic anomaly profiles reduced to the pole on top (blue line). S - southern line; C- central line; N - northern line (see location in Fig. 1).

Figure 5b

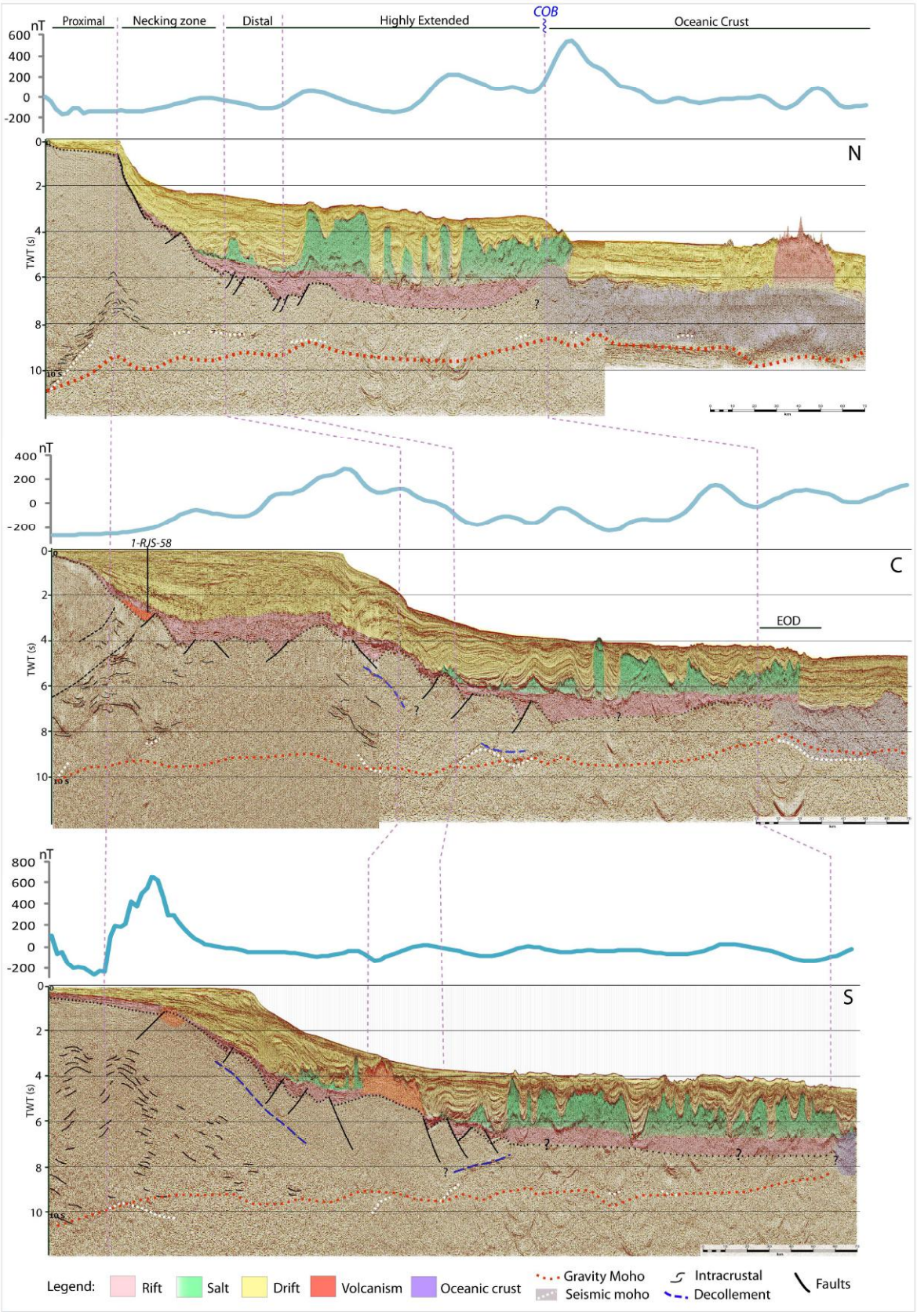
Proximal
Necking zone
Distal
Highly Extended
COB
Oceanic Crust
nT
600
400
200
0
-200
N
TWT (s)
0
2
4
6
8
10
10 s
C
1-R/S-58
EOD
800
S
Legend:
Rift
Salt
Drift
Volcanism
Oceanic crust
Gravity Moho
Seismic moho
Intracrustal
Decollement
Faults

Figure 6

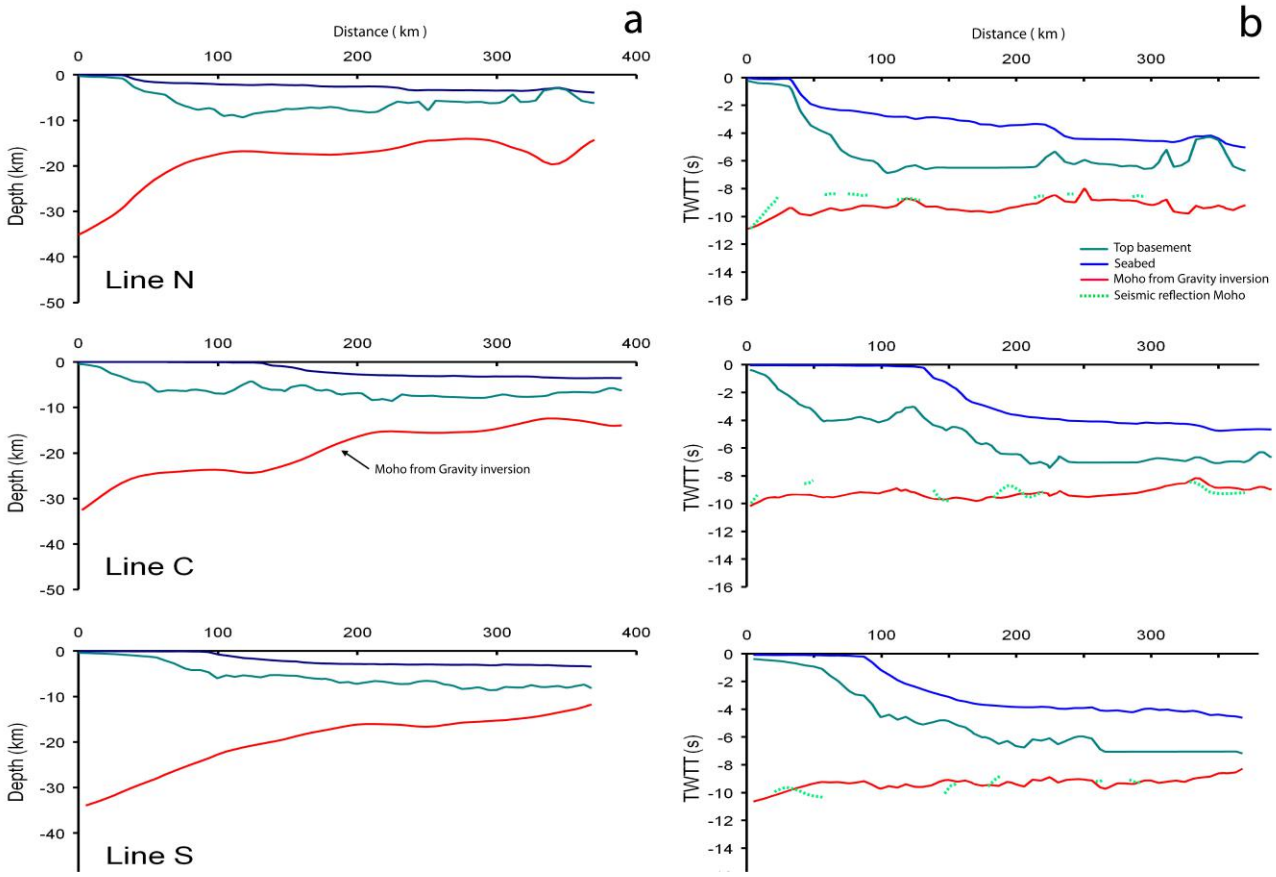

Fig. 6. (a) Cross-sections in depth for profiles N, C and S with Moho from gravity inversion using sediment thickness derived from seismic reflection data (Fig. 5) for profiles N, C and S. (b) Cross-sections in TWTT comparing Moho from gravity inversion with Moho seismic reflection interpretations.

Figure 7

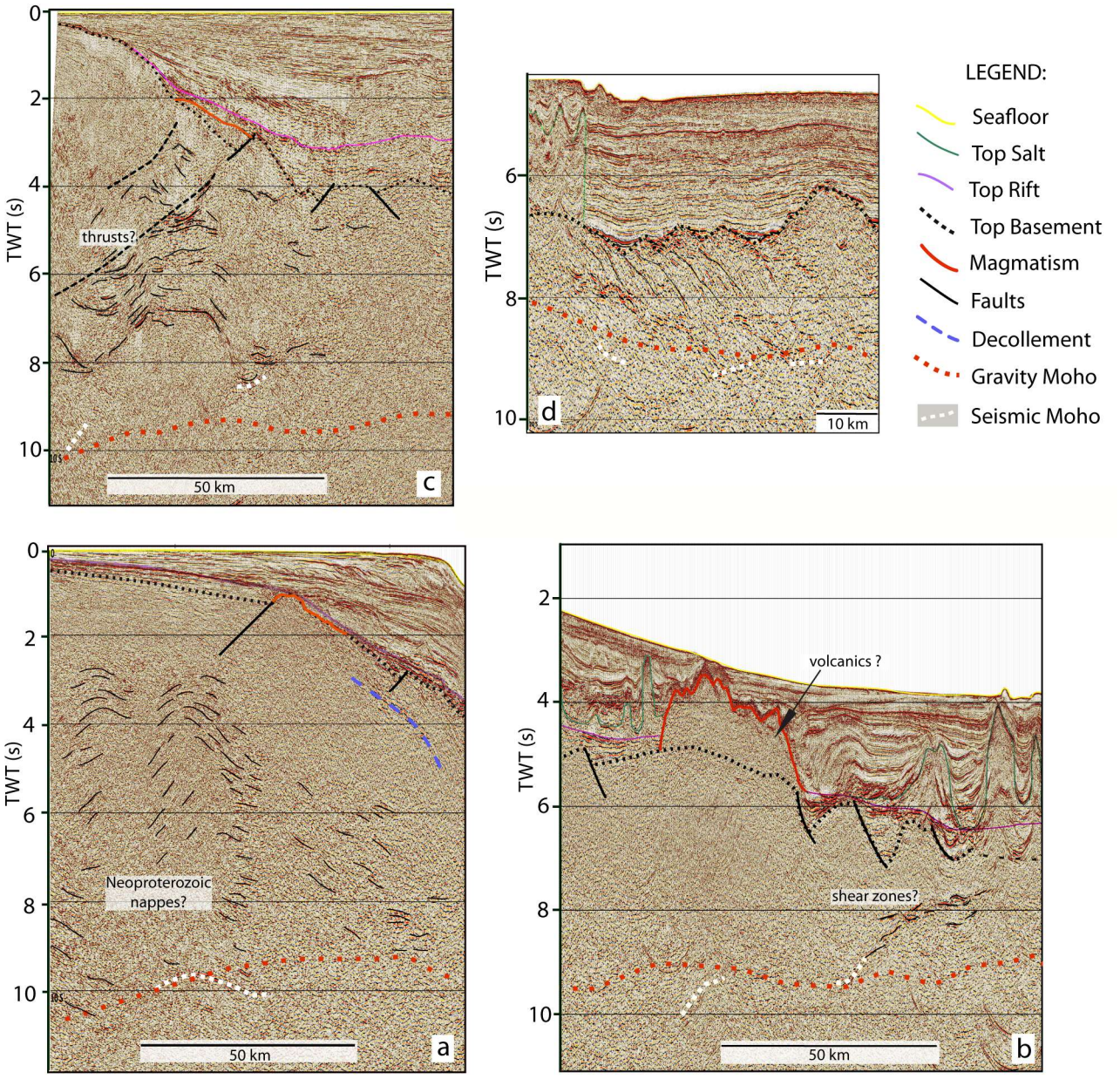

Fig. 7. Zoom of crustal structures of South (Section S) and Central Campos (Section C). a) Detail image of Section S showing basement volcanic beneath the CMH and two distinctive crustal reflection patterns: an upper massive crust and middle to lower crust displaying reflective basement, with large-scale concave-down reflectors; b) A structural high with reflection free seismic texture similar to a volcanic construction, and deep reflectors suggesting shear zones; c) Section C displays massive upper and reflective middle crustal layers, separated by discontinuities (dashed black lines); d) Detailed image of section C showing the embryonic oceanic crust.

Figure 8

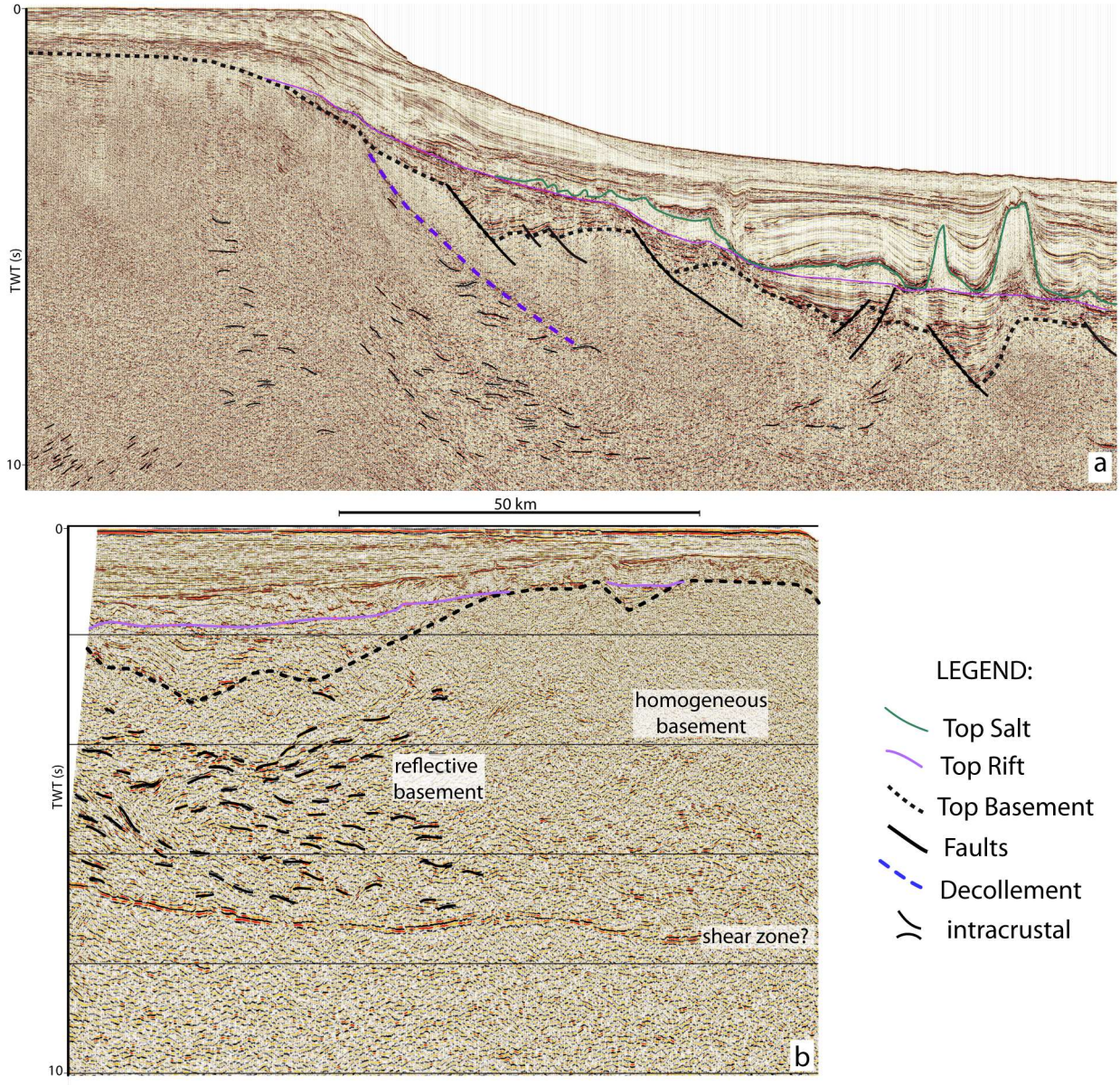

Fig. 8. a) Example of regional *decollement*, with large-scale block rotation, rooting at the brittle-ductile transition; b) strike line displaying the lateral contact between the reflective basement of CFTD and the homogeneous crust of the northern terrane (Araçuaí Belt?).

Figure 9

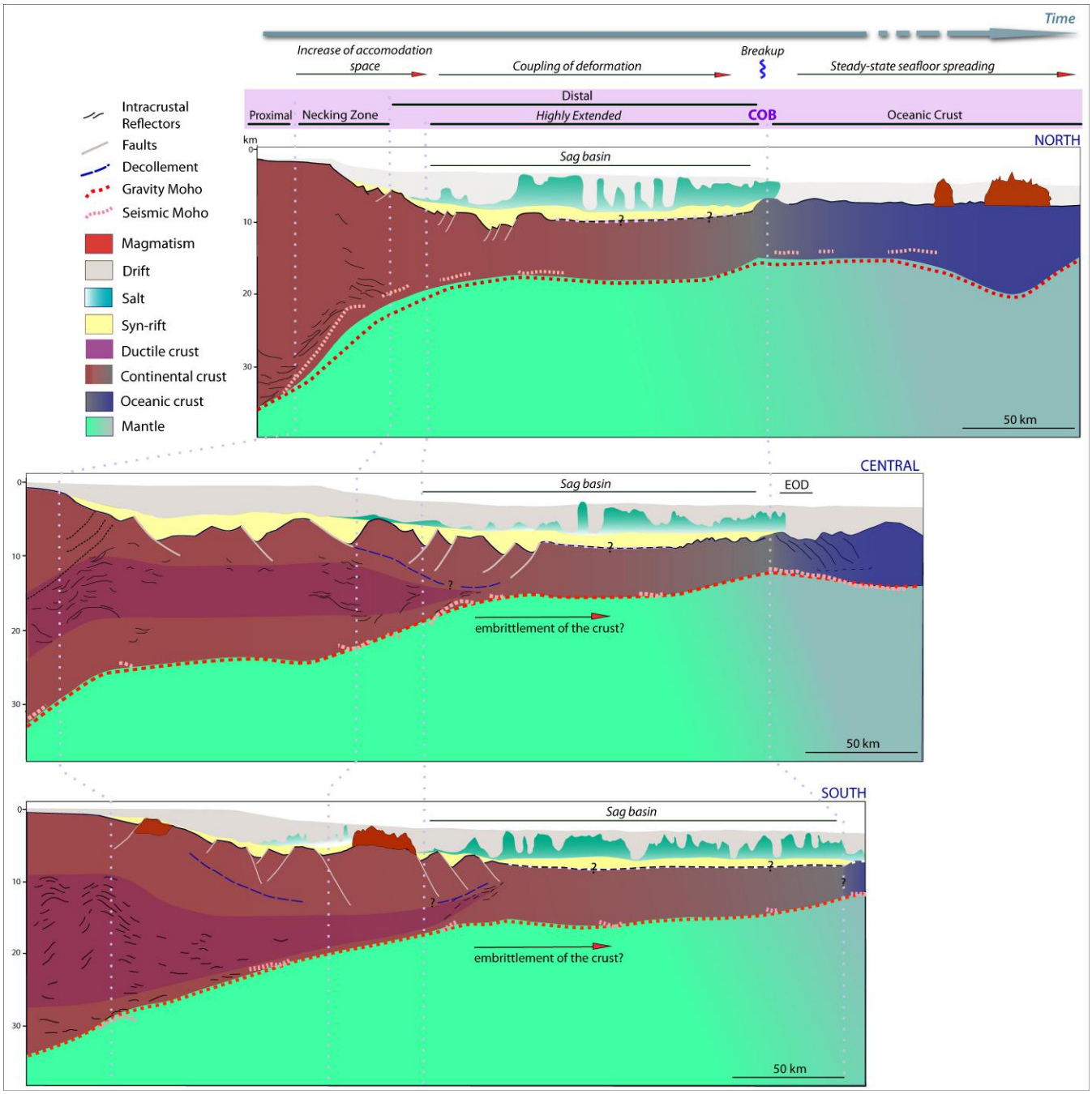

Fig. 9. Geological model illustrating the Campos Rifted Margin crustal architecture variation from north to south, the crustal domains and COB location. The three sections illustrate the main architectural types proposed in this study. EOD - Embryonic Oceanic Domain.

Figure 10

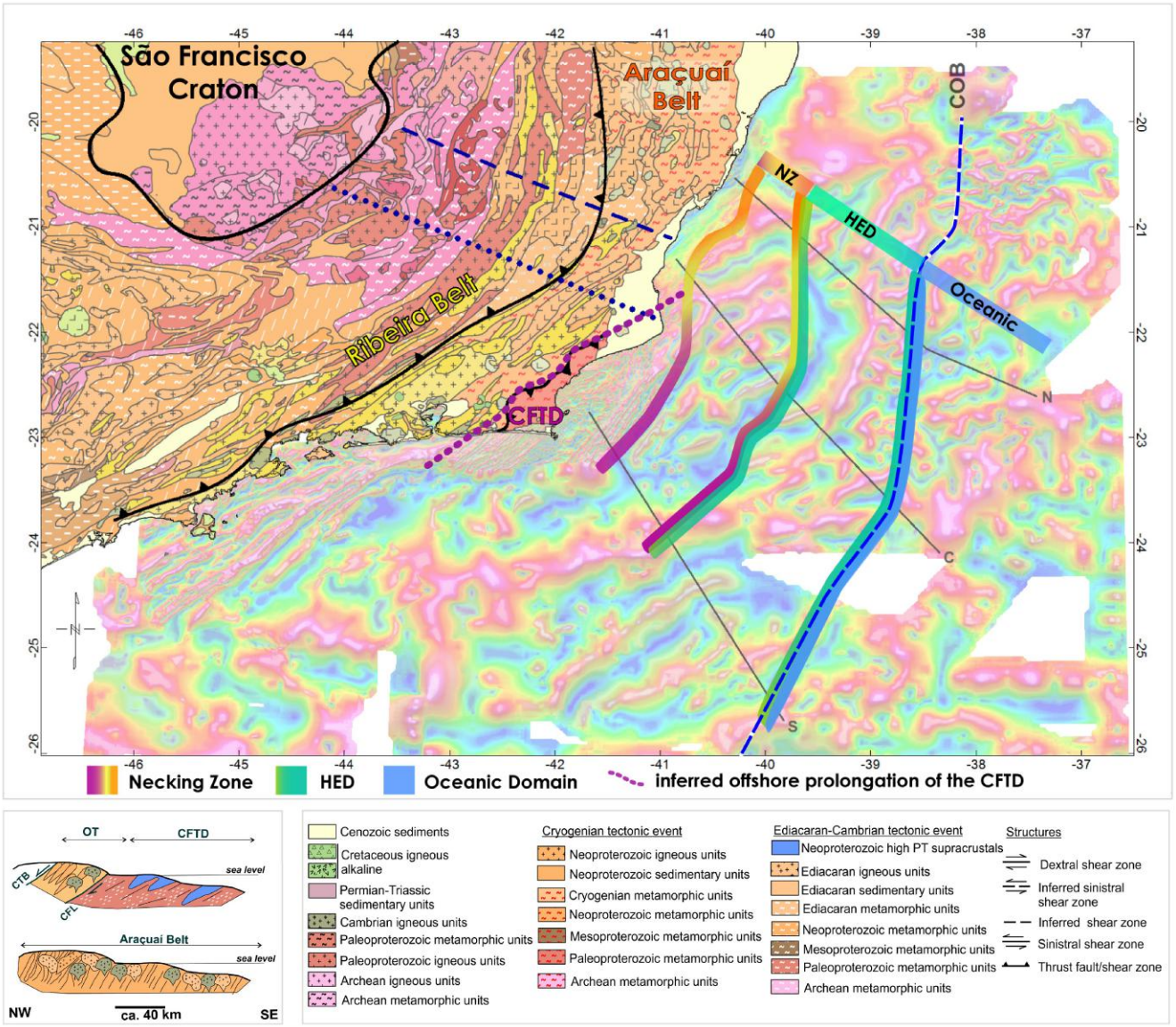

Fig. 10. The proposed Campos rifted margin domains and offshore prolongation of the continental terranes. Purple dotted line - offshore boundary of the CFTD. The color of the stripes along the margin represent the crustal basement variation. At the Necking Zone (NZ) the colors represent the transition between the CFTD (purple), Ribeira Belt (yellow) and Araçuaí Belt (orange) terranes, based on geophysical and geological data. Previous onshore boundaries are shown, based on seismic anisotropy variation (Assunção et al., 2004, blue dotted line); and geology (Ribeira - Araçuaí belts boundary of Heilbron et al., 2004, blue dashed line). Purple circles represent wells that reached the CFTD basement. The offshore background map is the tilt derivative of the magnetic anomalies and the onshore geology is from Schmitt et al. (2016).

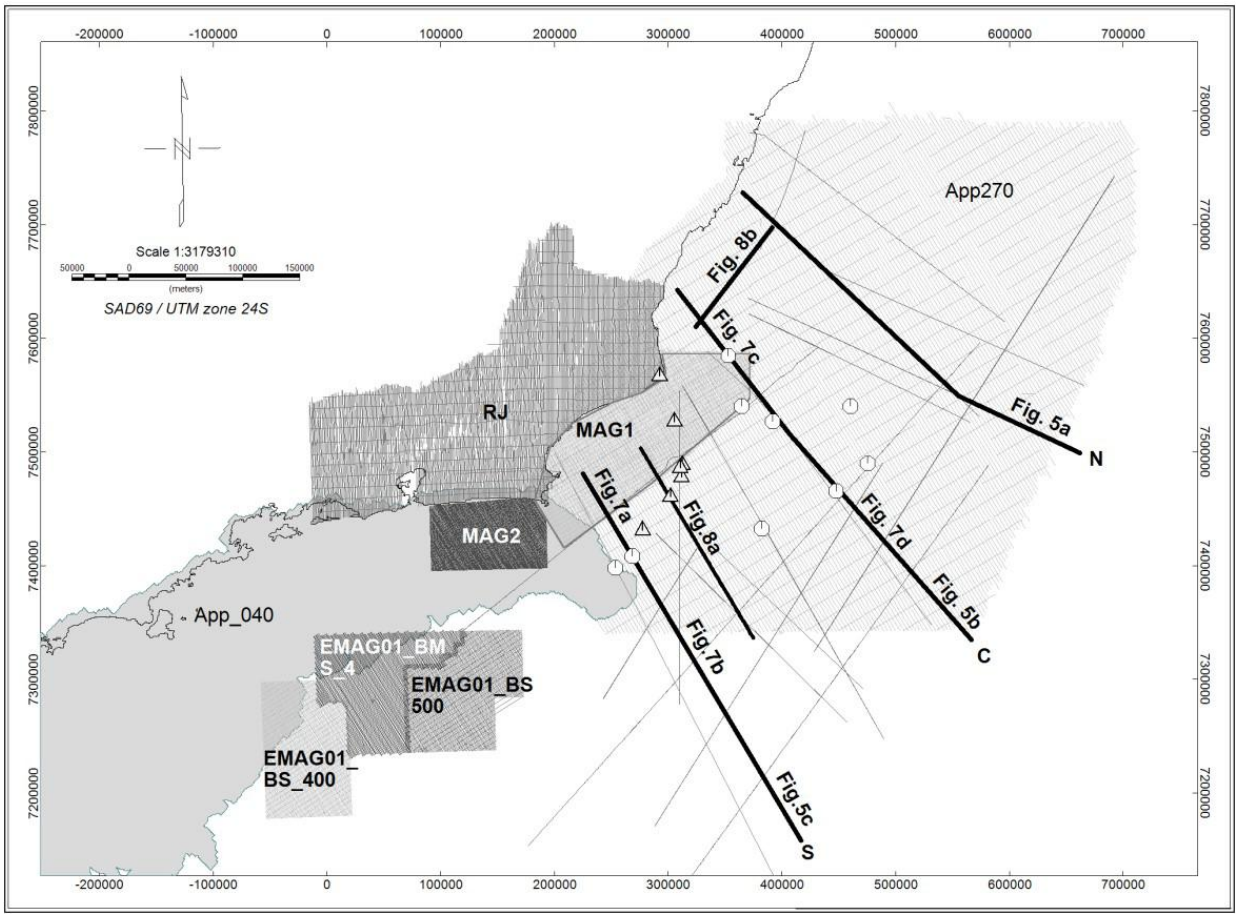

Fig. S1. Location of the aerosurvey acquisition areas for the magnetic data used in this study (see text for acquisition parameters) and the seismic sections shown in Fig. 5, 7 and 8.

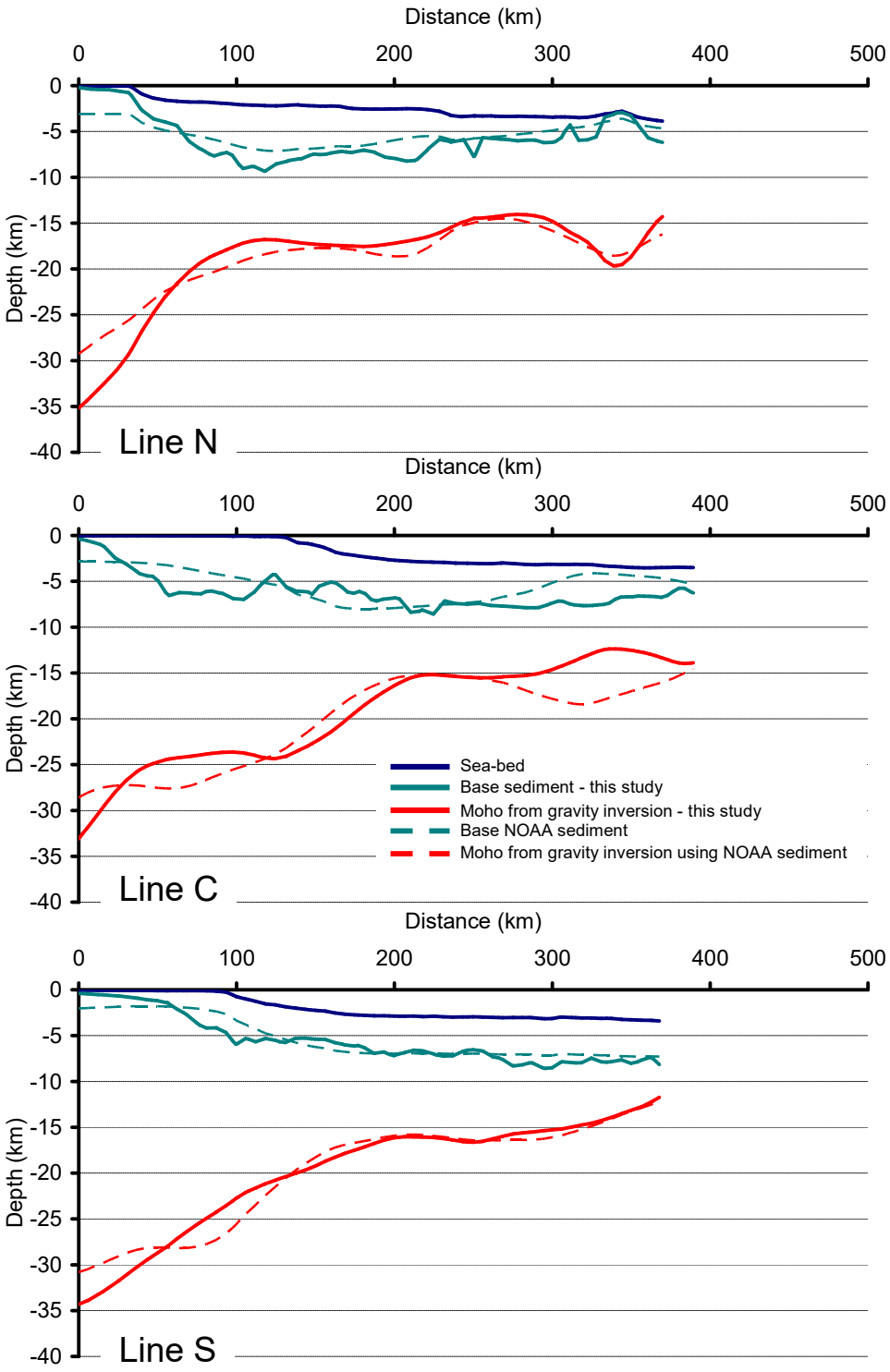

Fig. S2. Comparison of crustal cross-sections with Moho from gravity inversion for profiles N, C and S produced using public domain sediment thickness and that produced using sediment thickness derived from seismic reflection data (this study).

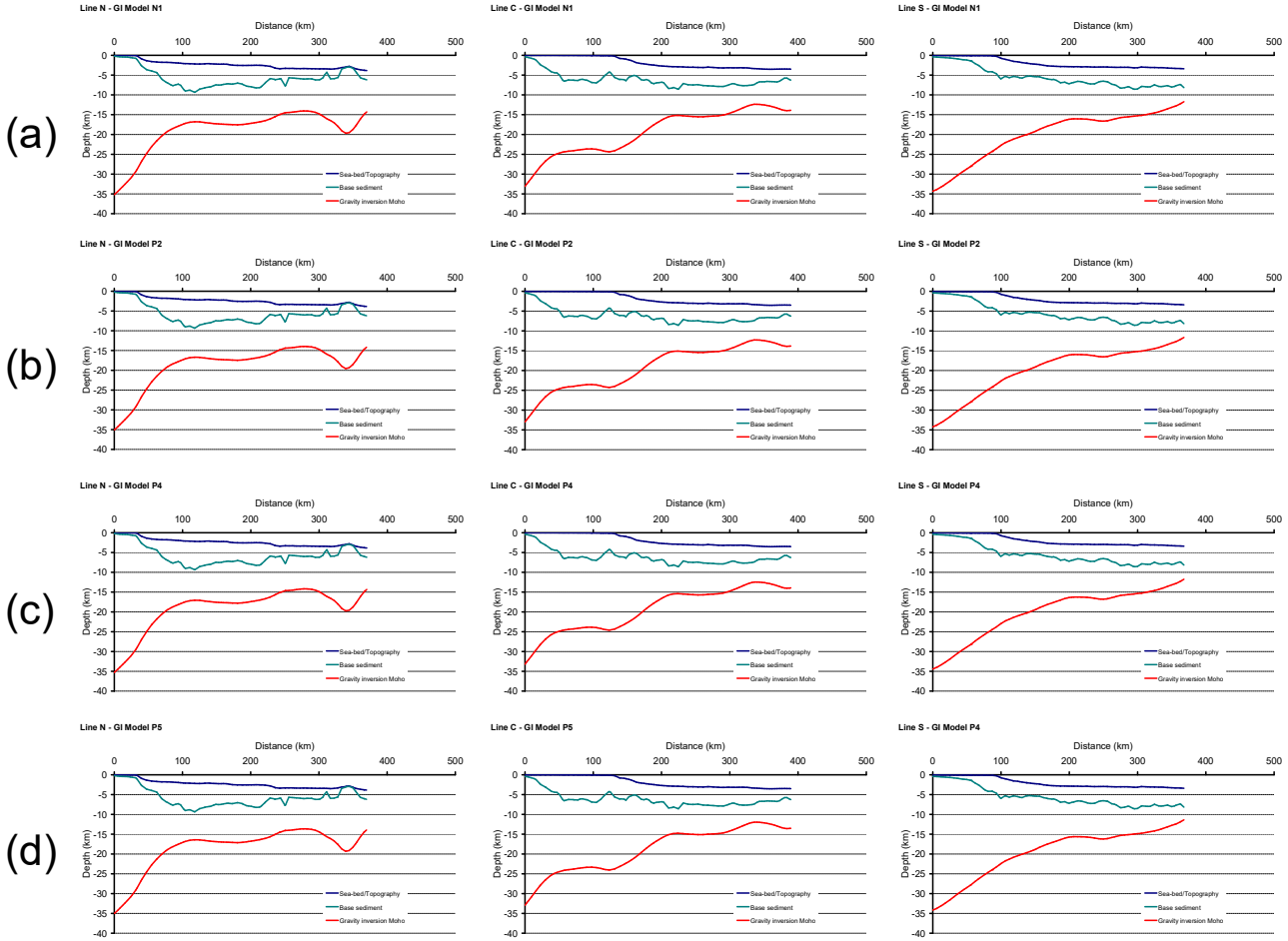

Fig. S3. Sensitivity tests of the application of ocean isochrons to condition the lithosphere thermal model used to determine the lithosphere thermal gravity anomaly correction. (a) & (b) use 110 Ma as the oldest isochron (and breakup age), (c) uses 120 Ma and (d) uses 100 Ma. (b) uses ocean isoschrons to define lithosphere cooling time (for thermal re-equilibration) and oceanic lithosphere thinning (1-1/β) equal to 1 (i.e. β =∞). (a), (c) and (d) use ocean isochrons to define lithosphere thermal cooling time only but with lithosphere thinning (1-1/β) determined from gravity inversion.